Xènia Fuentes Font

Polymeric replicas for biomedical applications and cell support

Final degree thesis

Supervised by Prof. Lluis F. Marsal and Dra. Pilar Formentín

Biomedical engineering degree

UNIVERSITAT ROVIRA I VIRGILI

Tarragona
2022

Table of contents

Summary

In this project, porous silicon has been used to work as a template with the aim to obtain polymeric surfaces to use them as a support for cell culture.

Microporous silicon samples, fabricated by electrochemical anodization process, were chemically modified via vapor deposition using a hydrophobic self-assembled monolayer (FOTS) to facilitate the peel-off of the polymers to obtain the corresponding replicas. We performed polymeric surface salinization by 3-aminopropyl triethoxysilane (APTES) with glutaraldehyde (GTA) followed by protein immobilization using collagen type I.

Morphological characterization of porous silicon substrates was carried out by Environmental Scanning Electron Microscope (SEM), contact angle technique was used to evaluate the functionalization and modification of polymeric replicas.

Those investigations were performed to determinate what is the ideal pore length in order to make replicas from it with different polymers and to get to the final objective, cell seeding.

1. Introduction

1.1. What is a biomaterial?

The definition of '*material'* has always been very broad: '*It is an element that can be transformed and grouped into a whole'*. We can therefore say that everything is made up of materials.

The discovery that initiated the process of creation and research of biomaterials was in the 19th century with the invention of plastics. Today, this technology focuses on developing novel polymers and composite materials, as they have shown that it is possible to obtain a material with optimal properties for a specific function.

The term "biomaterial" [1] refers to a substance that has been developed to interact with biological systems for either therapeutic (to treat, amplify, repair, or replace a tissue function of the body) or diagnostic purposes. Biomaterials is a field of study that is around fifty years old. Biomaterials science or biomaterials engineering are two terms used to describe the study of biomaterials. Over the course of its existence, it has grown steadily and strongly because of significant investments made by several businesses in the creation of new goods. The field of biomaterials science combines aspects of biology, chemistry, tissue engineering, and materials science.

Biomaterials may be classified according to their origin in natural or synthetic, amongst the natural ones we may find silk, wool, and collagen, whereas for synthetics -which are the most used we may find of metals, polymers, ceramics, and compounds.

Among the metals it is worth mentioning Silicon, a material that contains 92.2% of the isotope of mass number 28, 4.7% of Silicon-29 and 3.1% of Silicon-30, thus, Silicon resembles metals in their chemical behavior.

1.2. Porous Silicon

Porous Silicon (PSi) was unintentionally discovered in 1956 at the Bell Labs in the United States by Arthur Uhlir Jr. and Ingeborg Uhlir. The Ulhirs were working on a method for polishing and sculpting the surfaces of silicon and germanium at the time. [2]
But it was discovered that under several circumstances, a crude product in the shape of a thick black, red, or brown coating was developed on the material's surface. The results were merely stated in Bell Lab's technical notes at the time, with no further action taken.

It has revolutionized the silicon process by allowing photo and electroluminescence phenomena with relatively high efficiency in an indirect gap semiconductor. Since then, the PSi has given rise to two other small revolutions that have recently been associated: the biocompatibility of this material with various tissues and the ability to house materials with complementary properties in a nanostructured form. In this way, it makes it one of the best materials in the world, it is interesting to study how to work with this material and being able to observe its effectiveness.

1.2.1. Porous silicon fabrication

Nowadays, there are various techniques to produce PSi [3] such as:

1. **Stain etching:** The most direct, most expensive, and easiest method for creating PSi is stain etching. On an SOI wafer with a buried oxide layer that makes electrochemical etching challenging, it can be employed to create PSi. The primary drawback of this approach is that the thickness of the PSi layer has a maximum value [4] (about 1.5 m)[1].

2. **Photoetching:** PSi on SOI wafers, micromachined wafers, and wafers containing microelectronic circuits may all be manufacture using photoetching. The approach does not add any metallic contaminants to the substrate when HF solution is used in place of NaF and KF solutions [5]. This approach's biggest drawback is that it only functions with

[1] Stain etching under illumination should not be confused with photoetching.

n-type silicon wafers[2]. The second is that the achieved porous layer's thickness is not consistent [5].

3. **Metal-assisted etching:** One method of carrying out metal-assisted etching is to shape and deposit metal catalysts, then submerge the redeposited specimen in the HF and add oxidizing agent etchant. The alternative method involves submerging the unprocessed silicon wafer in a solution containing HF and various metal salts, such as potassium tetrachloroaurate (III), silver nitrate, and potassium hexachloroplatinate (IV) [6,7]. Here, the dissolving process is started by metal catalysts that have precipitated on the silicon surface.

4. **Vapor etching:** Vapor etching is overall an easy and affordable process. In solar cells when thin layers of PSi are required, it can be employed to make luminous silicon structures and antireflection coatings. To prevent the formation of Si/SiOx and ammonium hexafluoro silicate (NH4)2SiF6 nanoparticles instead of PSi, the concentration of the solution, temperature, and vapor etching time must all be accurately regulated. The process is unable to create very porous structures because the droplets' condensation causes a liquid film to develop on the surface, which removes the porous layer. As a result, if the specimen's area is too large compared to the container's diameter, the thickness and porosity will not be consistent [8,9].

5. **Reactive-ion etching**: The silicon atoms are removed from the silicon during the etching subsequence by SF6 ions and plasma radicals using a mix of chemical and physical etching methods. In this case, the pores are exposed to the O2 plasma during the oxidation subsequence, which causes a very thin oxide layer to form on their surface. The thin oxide layer is changed into a stable SiOxFy passivating film during the subsequent subsequence of fluorination, which replaces the dangling silicon/oxide interface bonds with SiF bonds. As a result of this, SiOxFy layer formation stabilizes the final porous chemical structure.

[2] It's not impossible to prepare p-type PSi by photoetching but the rate of the process it's not that good.

This has been repeatedly ben reported as a shortcoming of HF-based techniques used to create PSi structures [10,11]. By repeating these three subsequences, the PSi structures develop.

6. **Spark erosion:** Another early 1990s top-down method for fabricating PSi is spark erosion, which eventually went by the name spark processing. In addition to PSi, other porous materials, including as As, Bi, Ge, GaAs, Sb, Se, Sn, and Te [12,13], can also be produced using this technique. For at least a few hours, sparks are used to erode the silicon substrate into a tip shaped structure, leaving behind porous structures on the surface. The disintegration of silicon atoms during spark erosion is entirely physical and does not involve any chemical processes. The gaseous atmosphere is ionized by the discharges between the tip and the silicon substrate, and the silicon surface is then degraded by the collision of the ions.

7. **Laser-induced plasma erosion:** Regardless of the kind or quantity of the silicon wafers dopant, luminous MesoPSi-PSi has been created on both p-type and n-type silicon wafers via laser-induced plasma erosion. The layers' porosity ranges from 40 to 70 percent and their thicknesses may reach 500 nm. However, there is notable nonuniformity in the porous region's thickness, thus, depending on where the silicon target is in relation to the focal plane of the lens, the area of the porous zone may range from hundreds of micrometers to several millimeters [14].

8. **Oxidation of Rochow reaction byproduct:** By oxidizing the leftovers of the Rochow reaction, acid washing can create macropsia-PSi particles. To create a contact mass, metallurgical-grade silicon powders are ground with Cu-based particles. The resulting material is then used to create organosilicon compounds by reacting with chloromethane CH3Cl (Rochow reaction[3]). Unreacted silicon, metal complexes, and deposited carbon make up the waste contact mass byproduct. Porous Si/C composite is left behind after

[3] The Rochow reaction is the most common route to synthesise organosilane monomers in the chemical industry.

recovering the metal parts via acid washing. The anode in lithium-ion batteries has successfully been made using a porous Si/C composite. PSi can be produced by oxidizing the Si/C composite in air for one hour at 400°C [15,16,17].

9. **Ion implantation:** By using low-energy, high-dose ion implantation of silver into monocrystalline silicon wafers instead of a thermal annealing procedure, macro-PSi architectures may be created. More specifically, the implantation it performed at an energy of 30 keV and dosages more than $1x10^{16}$ cm^{-2} conditions at which pore development in most likely caused by a microexplosion and void clustering. Theoretically, a microexplosion may start a void and reduce the energy needed for the development further of surrounding voids; These voids may subsequently cluster together to reduce the density of dangling bonds. The manufactured porous layer features pores that are on average around 120 nm in size. Silver atoms have been seen to aggregate inside pore walls during ion implantation, resulting in nanoparticles with sizes ranging from 5 to 10 nm [18]. Although the optical behavior of the material is enhanced by the electromagnetic interaction between localized surface plasmon of silver nanoparticles and PSi structures, the presence of metallic nanoparticles is undesired in other application areas.

10. **Plasma hydrogenation:** A bottom-up strategy in which a thin coating of amorphous silicon (a-Si) with a thickness of around 200 nm is first deposited. To increase the number of voids, physical vapor deposition methods like as evaporation or sputtering are used to form the amorphous layer. The specimens are then put in a setup for DC hydrogen plasma-enhanced chemical vapor deposition (DC-PECVD). The hydrogenation is followed by a procedure called thermal annealing. The dangling bonds in the amorphous silicon layer are thought to be replaced by hydrogen radicals from the plasma during the hydrogenation process. The silicon surface is then thought to be passivated during the annealing step, and H2 is then thought to be exhausted from the specimen. A porous crystalline structure is created because of the energy released by the breakage of the Si–H bonds, which also encourages the rearranging of the specimen's silicon atoms [19]. Even though PSi can be created by performing one hydrogenation step followed by one annealing step, splitting the process duration into three consecutive repetitions of the

hydrogenation and annealing steps allows for more control over the characteristics of the porous layer that is created.

11. **Laser ablation:** This method uses a vacuum chamber to irradiate a silicon target with a pulsed laser beam. Placing the substrate close to the target where the ablation plume might reach allows for the collection of the laser-ablated silicon clusters. To improve the porous layer's adherence to the substrate, heat is often used. Besides to improve the homogeneity of the deposited coating, it is also rotated. The intensity of the incoming laser, the separation between the substrate and the target, and the length of the ablation may all affect how porous and thick the PSi layer is. Due of its incompatibility with existing technology, this approach has not received much attention for chip-based applications [20].

12. **High-density plasma deposition of silicon:** Homogeneous porous layers up to 1 m may be created on silicon wafers, glass and plastic substrates, metal foils, and surfaces coated with high-density plasma. The layer's void fraction and porosity are reduced by raising the plasma power [21] or by raising the temperature of the substrate. This bottom-up approach allows for porosities between 25 and 90 percent by adjusting substrate temperature and microwave power. The created PSi films exhibit luminescence in the red range and are water vapor sensitive.

13. **Oblique-angle deposition:** In order to create geometric shadowing, oblique-angle deposition is carried out by angling the substrate steeply with reference to the vapor stream. Shadow zones, where incident vapor flux cannot reach, are created as a result of random growth variation on the substrate surface. Greater height variations grow preferred as the process takes place, as a result, pores are left behind as an array of orientated nanorods [22]. The porosity may be customized by adjusting the vapor flux incidence angle during deposition. The surrounding amorphous silicon matrix encloses the material pores created by oblique-angle physical vapor evaporation processes. Such structures limit the uses of the material and damage the huge surface area of PSi that is

accessible. In fact, the preparation of antireflection coatings for solar cells has been the primary usage of this production method [22].

14. **Unidirectional solidification of molten silicon**: It has been possible to create porous cylindrical silicon ingots with elongated spheroidal "lotus-type" holes that are 25 mm in diameter and roughly 30 mm in height using unidirectional solidification of molten silicon in hydrogen environment [23]. The resulting ingots have an average pore size that is at least two orders of magnitude bigger than PSi structures made using conventional manufacturing methods [24].

15. **Porous silica reduction** A straightforward method for achieving PSi is porous silica reduction. This technique can produce all types of porosity [25]. To avoid the creation of silicon instead of magnesium silicate, the process must be carefully controlled. Other problems that may arise when using this technique include sintering and the return of oxygen, particularly in very porous materials [26].

16. **Dealloying:** Thin layers of meso-PSi with an ultrahigh density of cylindrical pores with an average diameter of 5 to 13 nm have been produced via the dealloying of Al-Si eutectic system. This is done by sputtering an Al0.56Si0.44 target at 0.1 Torr of Ar pressure and low temperatures (below 100°C), leading to Al-Si structure formation. The combination of nanoscale phase separation of the Al-Si system, during deposition, and subsequent removal of Al cylinders, by chemical etching, results in cylindrical pores [27,28]. In fact, the structural evolution of the Al-Si system that takes place at the surface during the film formation at low temperatures may be controlled by appropriately selecting the deposition parameters, particularly the deposition rate [29].

17. **Laser-induced silane decomposition:** High porosity mesoporous structures made of silicon nanocrystals have been created via this technique.

    Pulsed CO_2 laser induced SiH_4 breakdown in a sophisticated equipment has been used to create nanocrystals. The system consists of three vacuum chambers: an ultrahigh vacuum

(UHV) chamber housing the time-of-flight mass spectrometer, a differential chamber housing the size selection chopper, and a source chamber housing the flow reactor. The "source chamber" is a laser-driven CVD (chemical vapor deposition) reactor where SiH4 is pyrolyzed by pulsed CO_2 lasers to create silicon clusters. The reaction products are then retrieved through a conical nozzle aimed to the reaction area, perpendicular to both the gas flow and the CO_2 laser beam [30].

A "molecular beam" of non-interacting clusters is formed when the extracted nanocrystals are skimmed into a low-pressure vacuum chamber (differential chamber). The beam may be shifted vertically from the outside and is coordinated with the pulsed pyrolysis laser as it travels through the slits of a spinning chopper. Then to reduce the spread of cluster sizes, a tiny fraction of the originally wide cluster pulse is preselected using the chopper. Subsequently, a sample holder that may be positioned inside the cluster beam to capture the nanocrystals is located directly behind the helicopter. On the substrate, silicon particles of a chosen size can be placed. The silicon nanoparticles enter the UHV detecting chamber with a time-of-flight (TOF) mass spectrometer if the sample holder is moved out of the beam's path. When nanocrystals are gathered by the substrate, pores are immediately created [31]. Due to the inherent apparatus' intricacy and the porous layer's weak adherence, this method of production has not received much attention.

18. **Electrodeposition:** Galvanic deposition, commonly referred to as immersion plating, is another method for creating PSi structures. MesoPsi-PSi layers are formed on metallic substrates like pure aluminum or aluminum alloys by galvanic deposition when sodium hexafluoro silicic acid (Na2SiF6) is added to diluted hydrofluoric acid concentrated with nitric acid solution [32].

19. **Mechanical synthesis:** Large PSi matrices may be formed using this technique, which is not conceivable with using top-down production methods. The fundamental drawback of mechanical synthesis is lack of control over the shape of the pores, which is in addition to the restricted porosity. Additionally, there are a lot of contaminants in the mechanically produced matrix and a high defect density, both of which are significant problems [33]. In the ball milling step, the strong compressive stress caused by ball-powder-ball collisions

alters the Si–Si bond length, causes amorphization, and introduces many defects. The product has a substantially greater density of flaws and undesirable impurities than other PSi production processes, even though the structure recrystallizes, and most faults are eliminated during high-temperature treatment [34].

20. **Annealing of ultrathin films of amorphous silicon:** Rapid thermal annealing of redeposited ultrathin amorphous silicon layers can be used to create ultrathin low porosity silicon membranes [35].

21. **Sacrificial template:** for this ZnO nanowires are first produced in an array on the substrate. The specimen is then put into a CVD reactor where silane is used to cover the ZnO nanowires with silicon. The creation of PSi depends critically on the thickness of the over-coating silicon shell [27], which is regulated by the length of the silane exposure. In fact, porous nanotubes can only be produced in silicon with sidewall thicknesses of 12 nm or less. The silicon over-coating layer's crystallinity is determined by the temperature of the CVD process.

22. **Anodic etching,** which I am going to explain in more detail throughout this report since this is the method that we have used for our project.

1.2.1.1. Electrochemical etching

Over the past 60 years, the most popular technique for creating PSi has been anodic etching, also known as electrochemical etching. The simplest electrochemical cell used to anodize etch silicon is lateral cell. In this, the cathode electrode is made of graphite or any other conducting material resistant to hydrofluoric acid, while the cell body is built of acid-resistant polymers like PTFE (Polytetrafluoroethylene). The anode is a silicon wafer that is going to be etched.

Any silicon surface that is exposed to the electrolyte when the wafer is immersed in HF will become porous if the current density is below the critical level ($J < JPSL$). The simplicity and capability of the lateral cell to anodize silicon-on-insulator (SOI) wafers are its key benefits. Its main disadvantage is the unevenness of the resultant layer's porosity and thickness. The cause

of this inhomogeneity is a lateral potential drop across the wafer, which results in an uneven current density, which in turn causes an uneven porosity and thickness [35].

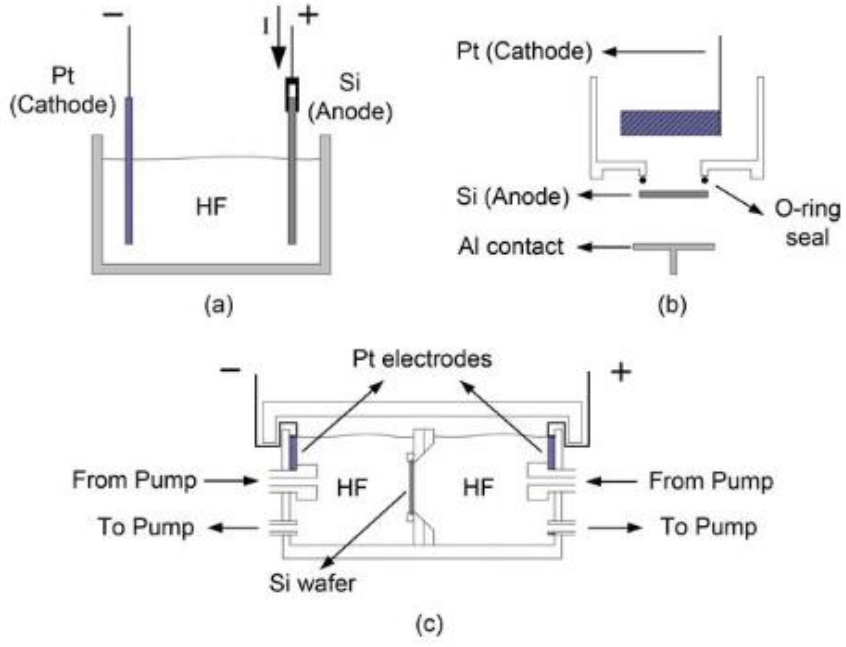

Figure 1. Different types of cells: (a) lateral cell, (b) single cell, (c) double cell

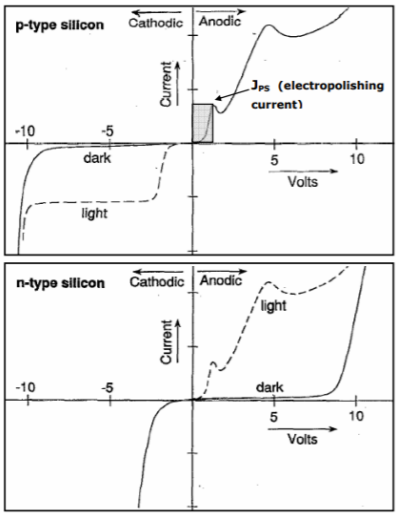

Figure 2. Typical i-V curves for silicon that has been doped with n- and p-types in aqueous HF. The dashed line depicts a reaction under illumination, whereas the solid line represents a response in the dark. The production of a surface anodic oxide, which is necessary for electropolishing, corresponds to the first (lower) current peak JPS. With the possibility for the creation of a second type of anodic oxide, the second (higher) current peak initiates steady current (potential) oscillations. The gray region illustrates the favorable regime for the synthesis of silicon that is porous.

1.2.2. Electrochemical reaction of PSi by anodization etching

The current at the silicon side of the silicon/electrolyte interface must be transported by holes and injected from the bulk towards the interface to generate PSi. Between zero and the electropolishing threshold, the current must be maintained. Depending on the doping level, external illumination of the sample is necessary to create a considerable hole current in n-type silicon. The anodization causes a gradual, total elimination of silicon if the current reaches the electropolishing threshold. The wafer then seems to be made of mirrors.

Although several theories explaining the chemistry of silicon dissolving have been put forward up to this point, it is widely agreed that holes are necessary for the development of pores and for electropolishing.

The semi-reaction that is formed during pore formation is as follows [36]:

$$Si + 6HF \rightarrow H_2SiF_6 + H_2 + 2H^+ + 2e^-$$

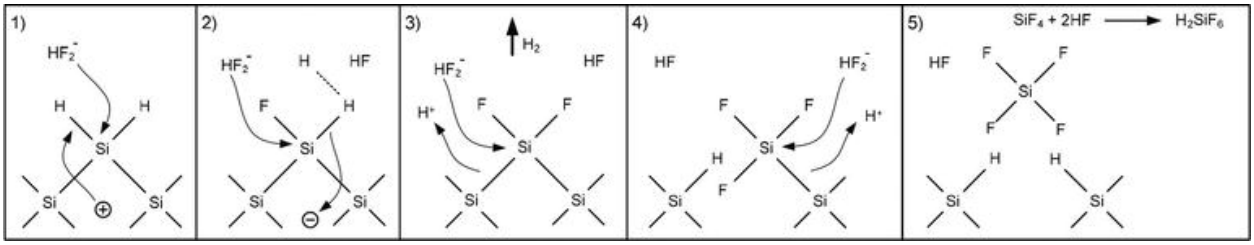

Figure 3. Divalent electrochemical dissolution of a silicon atom in hydrofluoric acid solution.

The final and stable product for silicon in HF is H2SiF6 or at least some of its ionized forms. In the following steps, during pore formation, only 2 of the 4 available silicon electrons participate in a charge transfer from the interface, while the remaining two are subjected to corrosive hydrogen formation.

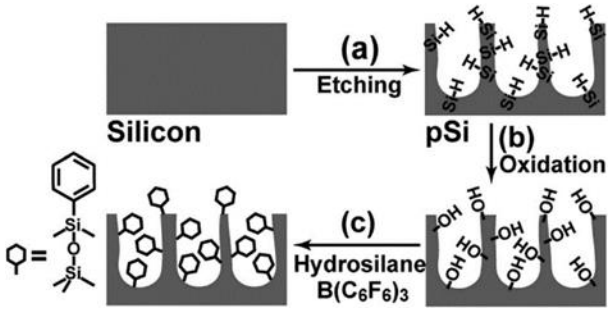

Figure 4. Pore formation

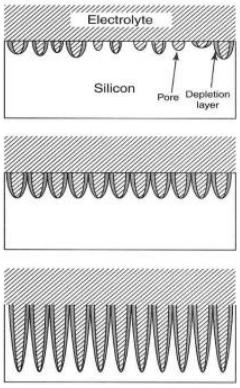

Figure 5. Pore formation

1.2.3. Features (pore morphology)

We can distinguish three categories regarding the pore dimension:

1. **Micropores**: < 2 nm
2. **Mesopores**: 2-50 nm
3. **Macropores**: > 50 nm

Pore characteristics such as form (smooth, branching, facetted, etc.), orientation, connectivity of pores, etc. are referred to as pore morphology. Because of the incredibly rich features of changes in pore size, shape, and spatial distribution, it is exceedingly challenging to comprehensively define the morphology of PSi. The pore morphology of microporous and MesoPSi may be characterized as having a sponge-like structure with densely and randomly branching pores that lack a distinct orientation. With a reduction in pore diameter, the tendency to branch rises. MacroPSi, in contrast, can have distinct pores with smooth walls, short branches, or dendritic branches.

The positive carriers (holes) involved in the electrochemical dissolution reaction are the cause of the pores' preferred growth in different directions. Dendritic pores are oriented in different directions, whereas pores with smooth walls often align to the location of holes.

1.2.4. Anodization parameters

Porous silicon fabrication by anodization has been used by several studies, getting a list of parameters that influence the formation process of the material. The essential parameters that modify properties of pSi are the following:

- Doping: Introducing impurities to a semiconductive material modulates its optical, electrical, and structural properties.
- Current density: Changes in the morphology and size of pores.
- HF concentration: Determines the range of current density values.
- Solvent where HF is diluted: PSi is hydrophobic, and the use of ethanol gives homogeneity to pore's growth due to the improvement in surface's wettability.
- Etching time: Affects the thickness of the layers.
- Illumination: Important for photosensitive substrates.

The porosity, thickness, pore diameter, and microstructure of PSi depend on these anodization conditions. In addition, there are other conditions that also have an effect, such as temperature, ambient humidity, and drying conditions.

Table 1. Summarize of anodization parameters and characteristics [35]

	Porosity	Etch rate	Critical current
HF concentration	↓	↓	↑
Current density	↑	↑	-
Anodization time	↑	Almost constant	-
Temperature	-	-	↑
Wafer doping (p-type)	↓	↑	↑
Wafer doping (n-type)	↑	↑	-

1.3. Applications of porous silicon

Porous silicon (PSi) has been used for device isolation because of its strong chemical reactivity and quick oxidation. It had already been employed for a variety of different tasks by the end of the 1980s. However, PSi did not get much notice until it was shown to have significant photoluminescence. PSi has been employed in the creation of several technologies, including flat panel displays, optical and acoustic filters, ultrasonic generators, distributed Bragg reflectors, biosensors, gas sensors, humidity sensors, and light-emitting structures [2].

1.3.1 Optic and optoelectronic applications

The material has received a lot of interest ever since Canham's publication on significant photoluminescence in PSi at ambient temperature in 1990 [37]. In fact, the interest generated by this finding is what has led to most of the knowledge we now possess about this subject. Radiative transition is made feasible in PSi by the quantum confinement effect, even though bulk silicon emits light poorly due to its indirect bandgap. Considering this, infrared, visible, and ultraviolet light emitting devices have been created. Additionally, PSi LEDs have been successfully combined with electrical components, raising the possibility of silicon-based monolithic optoelectronic integrated circuits [38].

PSi has also been used to produce several optical components. For instance, PSi layers with alternating low and high porosities have been used to create optical waveguides [39]. On these, total internal reflection would cause light to be trapped inside the low porosity layer, which has a greater refractive index than the neighboring low refractive index layers. The waveguide may handle many propagating modes depending on the layer thickness and refractive indices [39].

Despite being steered inside a layer with limited porosity, light may be coupled into and out of a waveguide thanks to fading fields in the layers above and below. Other optical uses for PSi include diffraction gratings, optical resonators, and photonic crystals [39,40].

1.3.2. Electronic applications

The primary uses for PSi in the realm of electronics are gas sensing, gettering, lithium-ion batteries, and antireflection coatings for solar cells. PSi is a viable choice for the implementation of gas sensors due to the substantial surface area. Based on the modification of the material's electrical and optical properties in the presence of more than 50 chemical species, almost a dozen designs have been proposed for PSi gas sensors. In lithium-ion batteries, PSi has also been used as an anode. These anodes are superior to traditional lithium-ion battery anodes in terms of capacity and lack mechanical instability because of the problem with bulk silicon's expansion and contraction brought on by the lithiation and delithiation processes [41].

Gettering, or the expulsion of impurities from the active areas of electronic devices, is another area where PSi has electronic applications. PSi has a large surface area that allows it to absorb contaminants, making it an ideal getter medium [42]. The adjustable refractive index of PSi makes it a suitable choice for use as antireflection coatings in solar cells [43].

1.3.3. Medical and diagnostics applications

For medical and diagnostics applications, PSi structures that are independent of chips have also been used. Proteins, enzymes, and antibodies may all be detected using biosensors. To diagnose prostate cancer, PSi has been used to assess the prostate-specific antigen (PSA). This substance has also been used to treat cancer by brachytherapy, which involves inserting radioactive implants directly into the target area. In this method, a medical radioisotope is injected into the tissue that must be destroyed while being housed in a PSi capsule.

Preclinical testing is now being done on biodegradable PSi for drug delivery, furthermore, PSi has been proposed as a viable choice for this nanocarrier technology due to the material's configurable pore size and modifiable surface chemistry, which enable customizable drug load and release [44].

Finally, due to its beneficial qualities, PSi might be taken into consideration for tissue engineering. In this type of regenerative medicine, the body is given a temporary biodegradable scaffold so

that the surrounding tissue may repair naturally. As a result, the scaffold [45] should be constructed from a biocompatible substance that is simple to produce, shape, and disintegrate under control.

Other applications of the porous silicon are shown in table 2.

Table 2. Porous silicon applications [35].

Application area	Role of PSi	Key property
Optoelectronics	1. LED 2. Waveguide 3. Field emitter 4. Optical memory	- Efficient electroluminescence - Tunability of refractive index - Hot carrier emission - Non-linear properties
Micro-optics	1. Fabry-Pérot 2. Photonic bandgap structures 3. All optical switching	- Refractive index modulation - Regular macropore array - Highly non-linear properties
Energy conversion	1. Antireflection coatings 2. Photo-electrochemicals cells	- Low refractive index - Photocorrosion cells
Environmental monitoring	Gas sensing	Ambient sensitive properties
Microelectronics	1. Micro-capacitor 2. Insulator layer 3. Low-k material	- High specific surface area - High resistance - Electrical properties
Wafer technology	1. Buffer layer in heteroepitaxy 2. SOI wafers	- Variable lattice parameter - High etching selectivity
Micromachining	Thick sacrificial layers	Highly controllable etching
Biotechnology	1. Tissue bonding 2. Biosensor	- Tunable chemical reactivity - Enzyme immobilization

1.4. Polymers

Any member of the family of natural or artificial substances known as polymers is made up of very big molecules, or macromolecules, which are variations of simpler chemical building blocks known as monomers. Numerous components of living things are made of polymers, such as proteins, cellulose, and nucleic acids. They also serve as the building blocks for materials manufactured by humans, including concrete, glass, paper, plastics, and rubbers, as well as minerals like diamond, quartz, and feldspar.

The term "polymer" refers to an arbitrary number of monomer units. When there are a lot of monomers, the mixture is sometimes referred to as a high polymer. Monomers of the same molecular weight, shape, or chemical make up are not required for polymers to form. One type of monomer makes up some natural polymers. However, the majority of polymers, both natural and manmade, are composed of two or more different kinds of monomers; these polymers are referred to as copolymers.

1.4.1. Types of polymers

Organic

Living creatures depend on organic polymers for fundamental structural components and participation in essential life activities. For instance, polymers make up all of the solid components of plants. Among them are cellulose, lignin, and other resins. A polymer made of sugar molecules is called a polysaccharide, which is what cellulose is. A complex three-dimensional network of polymers makes up lignin. Isoprene, a simple hydrocarbon, is a component of wood resins. Rubber is an additional well-known isoprene polymer.

Inorganic

Diamond and graphite are two examples of the numerous inorganic polymers that may be found in nature. They both contain carbon. The three-dimensional network of links between the carbon atoms in diamond is what gives the substance its hardness. The carbon atoms join in graphite, which is used as a lubricant and in pencil "leads," in planes that may glide past one another.

Synthetic

Different kinds of processes can result in the production of synthetic polymers. By adding one monomer after another to the expanding chain, several common simple hydrocarbons, including ethylene and propylene, may be converted into polymers. A compound polymer, polyethylene is made up of ethylene monomers that are repeated. It might include up to 10,000 monomers

connected by lengthy, coiled strands. Crystalline, transparent, and thermoplastic, polyethylene softens at high temperatures. It is employed in the production of bottles and containers as well as for packing, molding, and coating. Although it is tougher than polyethylene, polypropylene is likewise crystalline and thermoplastic. Between 50,000 to 200,000 monomers might make up its molecules. This substance is used to create molded products and in the textile industry.

1.4.2. Polymer Chemistry

Polymer chemistry is the field that studies these materials. Biochemistry and the study of natural polymers share many similarities, but polymer chemists face particular challenges in the synthesis of novel polymers, the study of polymerization mechanisms, and the characterisation of the structure and properties of polymeric materials.

Polymers with different degrees of flexibility, solubility in water, hardness, and biodegradability have been created by polymer scientists. They have developed polymeric materials that are as durable as steel while being lighter and more corrosion-resistant. Pipelines for water, natural gas, and oil are now frequently built using plastic pipe. In order to create lighter, more fuel-efficient automobiles, automakers have increased the usage of plastic components in recent years.

1.4.3. Biopolymers

Biopolymers are organic materials produced by the cells of living things. Monomeric units that are covalently bound together to create bigger molecules make up biopolymers. Polynucleotides, polypeptides, and polysaccharides are the three primary groups of biopolymers, which are categorized based on the monomers employed and the structure of the biopolymer generated. Long polymers made of 13 or more nucleotide monomers are known as polynucleotides and include RNA and DNA.

PDMS

A class of polymeric organosilicon compounds known as silicones includes polydimethylsiloxane (PDMS), usually referred to as dimethylpolysiloxane or dimethicone. Due to its adaptability and numerous uses, PDMS is the most popular silicon-based organic polymer.

It is renowned in particular for having peculiar rheological (or flow) characteristics. PDMS is optically transparent, inert, non-toxic, and non-flammable in general. It belongs to a variety of

silicone oils (polymerized siloxane). It is used in a variety of products, including elastomers, medical equipment, contact lenses, shampoos (because it makes hair lustrous and slippery), food (as an antifoaming ingredient), caulk, lubricants, and heat-resistant tiles.

PGLA

Due to its biodegradability and biocompatibility, PLGA, also known as poly(lactic-co-glycolic acid), is a copolymer that is employed in a variety of therapeutic devices that have received FDA approval. By ring-opening co-polymerizing glycolic acid and lactic acid cyclic dimers, also known as 1,4-dioxane-2,5-diones, two distinct monomers, PLGA is created.

1.4.4. Interactions

The interactions that various biopolymers have with other polymers determine how important such interactions are to the live organism. Covalent bonds between polymers can occasionally be found, as in the proteoglycans found in animal connective tissue or the lignin and polysaccharides found in plant cell walls. However, noncovalent interactions, which include weaker connections like hydrogen or ionic bonding or hydrophobic associations, occur far more frequently. Because a region of the surface of one polymer molecule fits perfectly (sometimes after small conformational changes) onto the surface of another, even if the bonding is relatively weak, the interactions can be powerful.

Since enzymes are involved in the manufacture and breakdown of all biopolymers, proteins must be able to interact with other polymers. However, relationships between nonenzymic proteins and other proteins, polysaccharides, or nucleic acids are well documented. For instance, intricate connections between many proteins (myosin, actin, troponin, and tropomyosin) are responsible for and regulate muscle movement, whereas collagen fibers are connected to both glycoproteins and proteoglycans in connective tissues. While polypeptide hormones must be recognized by their receptors, which are either proteins or glycoproteins, protein antibodies can attach to protein or polysaccharide antigens.

Repressors are an example of a protein that interacts with nucleic acids by binding to certain secondary structures or base sequences on polymeric acids. The protein molecules that attach to these base sequences frequently include two subunits so that one may bind to either strand of

the DNA. In certain situations, these base sequences are practically palindromic (read the same backward or forward) as in XV.

2. Working hypotheses and objectives

Once these concepts have been presented, we move to the practical portion of this work, where we will use our expertise and laboratory tools to support research into polymeric replicas for biomedical applications and cell support. We will then extract some results for evaluation and discussion.

Our objectives are the following:

1. Achieving the creation of microporous Macro-PSi by anodic etching method and making homogeneous porous throughout the sample. To achieve that, we want to get to know which voltage and/or necessary time (or which one of the two variables is better to make changes) we need for these wells to follow the most homogeneous throughout the sample. Hypothesis 1: We are going to try the electrochemical anodization with short times, from 20 minutes to 5 minutes, and with that, our wells should have a maximum profundity of 2 μm. If the surface has larger wells, once we want to make our replicas, those are not going to be homogeneous, and we do not want that.
2. From the macro-Psi surfaces, make mirrored replicas with PDMS and at the same time make all these replicas equal. With the PDMS surfaces, make mirrored replicas with the other polymer, PGLA, and at the same time ensure that all these replicas are equal.
3. Choose which is the best PDMS replica (considering its homogeneity) of all the ones we make and functionalize it with APTES and GTA in order to attract cells in future studies.
4. In addition, we will try other forms of Macro-PSi and try to make replicas of them and observe them.

3. Methodology

3.1. Variables and resources

3.1.1. Equipments

Porous silicon set-up

The porous silicon used in this work was fabricated by electrochemical anodization method in presence of a hydrofluoric acid (HF) solution at different concentrations. The experimental setup is shown in Figure 6.

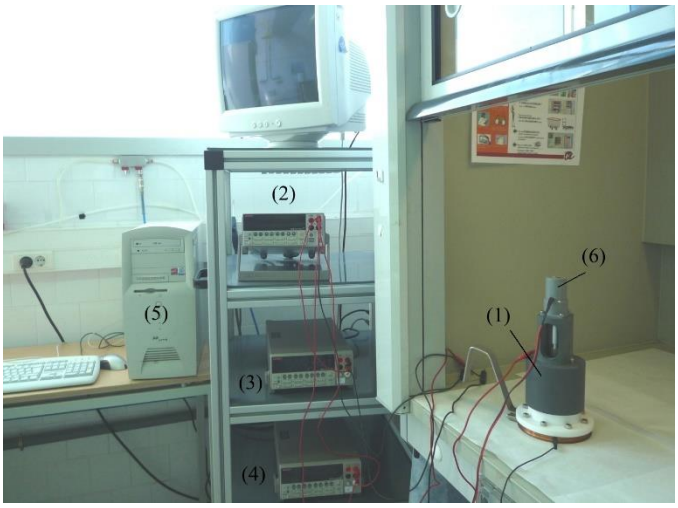

Figure 6. Porous silicon set-up

Polytetrafluoroethylene (PTFE or Teflon), which resists HF even at high concentrations, was used to make our cell. The cell body is a cylindrical-section receiver that makes it easier for the stirrer to renovate the electrolyte. In addition, the walls of the hole at the bottom of the receiver where the electrolyte comes into touch with the wafer are inclined rather than vertical to make it easier to renovate the electrolyte and remove the hydrogen bubbles from the wafer's surface. With the cell's volume regulated, the least amount of electrolyte feasible has been stirred.

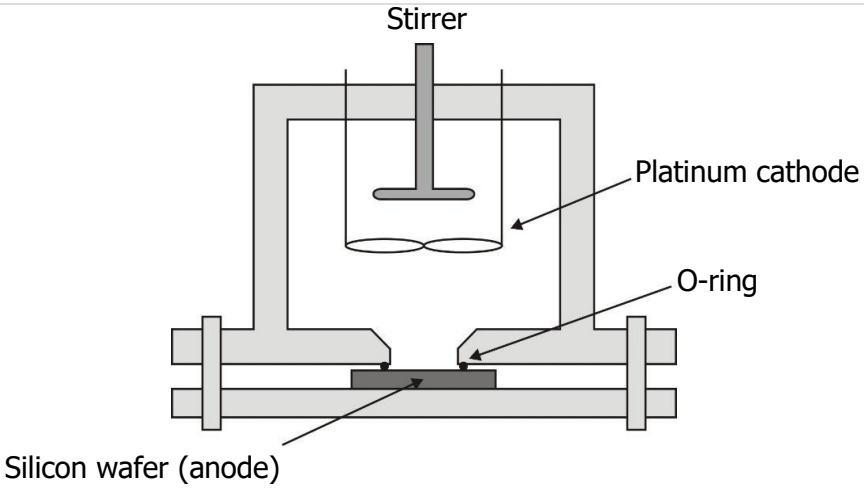

Figure 7. Scheme of the electrochemical cell for PSi fabrication [36].

The wafer is positioned near the bottom of the cell so that bubbles created on the surface can be eliminated by the actions of the stirrer and gravity. By pushing the wafer against a vinylidene fluoride-hexafluoropropylene (Viton®) O-ring, the cell is sealed. The sample region that will be exposed to the electrolyte is defined by the O-ring seal.

The backside contact of the wafer is a copper disk which enables a uniform contact on the whole area of the wafer. Due to the high resistivity (low doped) of the wafers used a thin gold layer of some tens of nanometers were deposited in the back surface of the wafers to provide a good contact between the wafer and its back-side metallic connection (copper disk).

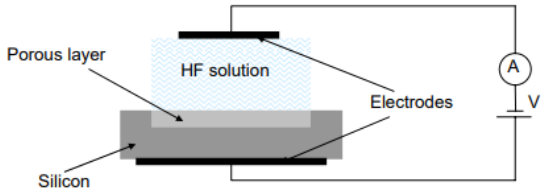

Figure 8. Scheme of the electrochemical cell for PSi fabrication [35].

The stirrer is mechanic, and its shape has been specially selected to stir the electrolyte from bottom to top. The stirrer rotates because of a continuous motor. The rotation velocity is selected by adjusting the voltage applied to the motor.

The process of pore growth can be realized either by controlling the anodic current or the potential. The most widely used method is the current control, because it allows a better control of thickness and reproducibility of the PSi. For our fabrication system we have

realized current control using a Keithley 2420 SourceMeter. This source enables a perfect control of the time and current applied during the growth. Two multimeters are used for the measurement of the current and the voltage of the system during the etching process [28].

Morphological Characterization

SEM: A concentrated electron beam is used to scan a sample's surface in a environmental scanning electron microscope (SEM), which creates pictures of the sample. The sample's surface topography and chemical composition are revealed by the signals that are created because of the electrons' interactions with the sample's atoms. A picture is created by combining the position of the electron beam with the strength of the signal being detected as it is being scanned in a raster scan pattern. A secondary electron detector is *used* in the most popular SEM mode to find secondary electrons released by excited atoms (Everhart–Thornley detector).

Figure 9. SEM microscopy

The topography of the specimen is one factor that affects the number of secondary electrons that may be detected and, consequently, the signal strength. The resolution of certain SEMs can exceed 1 nm.

Specimens are examined at a variety of cryogenic or high temperatures using specialist equipment, as well as under high vacuum in a standard SEM or low vacuum or wet conditions in a variable pressure or environmental SEM [46].

Chemical Characterization

Theta Optical Tensiometer (Attension): Each PSi, PDMS, and PGLA surface's hydrophobicity was assessed by measuring the water contact angle using a Theta Optical Tensiometer (Attension, Finland). In a nutshell, 10 µl of water was dropped onto several PDMS surfaces, and the contact angles were determined using the Drop Shape Analysis software's static sessile drop tangent approach. The angle produced between the substrate surface and the tangent to the drop surface was described as the contact angle. For each PSi, PDMS, and PGLA substrate, at least three places of contact were examined [47].

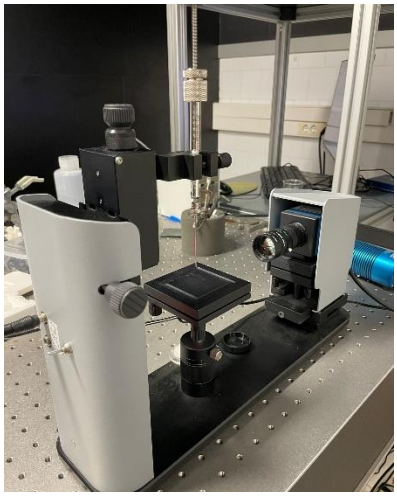

Figure 10. Theta Optical Tensiometer

3.1.2. Chemicals

Chemical anodization PSi

Table 3. Chemicals used in Chemical anodization PSi

Name of the chemical	
HF	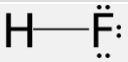 Dihydrogen fluoride, often known as fluorane, is an inorganic substance having the formula HF. The main industrial source of fluorine is this colorless gas or liquid, which is frequently an aqueous solution known as hydrofluoric acid. It serves as a crucial raw material in the production of several crucial substances, such as medications and polymers like polytetrafluoroethylene (PTFE). In the petrochemical sector, HF is frequently employed as a superacid component. In comparison to other hydrogen halides, hydrogen fluoride boils at a temperature close to that of ambient air. Upon coming into touch with moisture, the exceedingly hazardous gas hydrogen fluoride transforms into the corrosive and penetrating hydrofluoric acid. The quick deterioration of the corneas by the gas might potentially result in blindness [48].
DMF	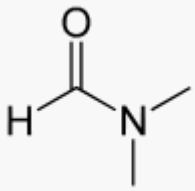 An organic substance having the formula (CH3)2NC(O)H is dimethylformamide. Commonly referred to as DMF, this colorless liquid is miscible with water and most organic liquids (although this initialism is occasionally used for dimethylfuran, or dimethyl fumarate). Chemical processes frequently use DMF as a solvent. Although dimethylformamide has no scent, technical-grade or damaged samples sometimes have a fishy smell because to a dimethylamine contaminant. Impurities that cause dimethylamine degradation can be eliminated by sonicating samples at low pressure or sparging samples with an inert gas like argon. It shares structural similarities with formamide, as suggested by its name [49].

Chemical modification of the porous silicon

Table 4. Chemicals used in Chemical modification of the PSi

Name of the chemical	
Trichloro(3,3,4,4,5,5,6,6,7,7,8,8,8-tridecafluorooctyl)silane (FOTS)	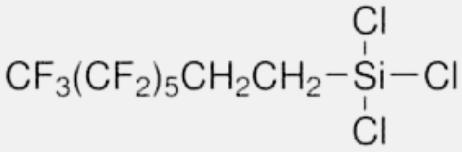

Fabrication of polymeric replicas with PDMS PSi

Table 5. Chemicals used in the Fabrication of polymeric replicas with PDMS PSi

Name of the chemical	
Polydimethylsiloxane	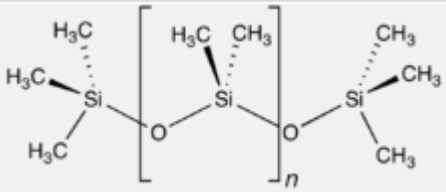 A class of polymeric organosilicon compounds known as silicones includes polydimethylsiloxane (PDMS), usually referred to as dimethylpolysiloxane or dimethicone. Due to its adaptability and numerous uses, PDMS is the most popular silicon-based organic polymer. It is renowned for having peculiar rheological (or flow) characteristics. PDMS is optically transparent, inert, non-toxic, and non-flammable in general. It belongs to a variety of silicone oils (polymerized siloxane). It is used in a variety of products, including elastomers, medical equipment, contact lenses, shampoos (because it makes hair lustrous and slippery), food (as an antifoaming ingredient), caulk, lubricants, and heat-resistant tiles [50].

Fabrication of polymeric replicas with PGLA PSi

Table 6. Chemicals used in the Fabrication of polymeric replicas with PGLA PSi

Name of the chemical	
Poly(lactic-co-glycolic acid)	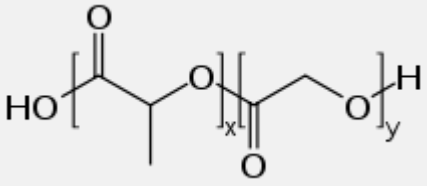

	Due to its biodegradability and biocompatibility, PLGA, also known as poly(lactic-co-glycolic acid), is a copolymer that is employed in a variety of therapeutic devices that have received FDA approval. By ring-opening co-polymerizing glycolic acid and lactic acid cyclic dimers, also known as 1,4-dioxane-2,5-diones, two distinct monomers, PLGA is created. Additional polymer qualities can be added by the synthesis of random or block copolymers. Tin(II) 2-ethylhexanoate, tin(II) alkoxides, or aluminum isopropoxide are often employed catalysts in the production of this polymer. In PLGA, subsequent monomeric units (of glycolic or lactic acid) are connected by ester linkages during polymerization, producing a linear, aliphatic polyester as a byproduct [51].
DCM	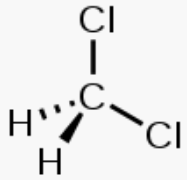 The chemical name for dichloromethane (also known as DCM, methylene chloride, or methylene bichloride) is CH2Cl2. This colorless, flammable liquid, which has a pleasant, chloroform-like aroma, is frequently employed as a solvent. It is polar and miscible with a variety of organic solvents despite not being miscible with water [52].

Functionalization of polymeric surfaces

Table 7. Chemicals used in the Functionalization of polymeric surfaces

Name of the chemical	
Ethanol	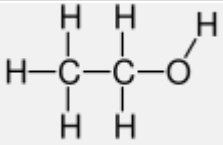 An organic chemical molecule, ethanol is also known as ethyl alcohol, grain alcohol, drinking alcohol, or just alcohol. With the chemical formula C2H6O, it is a straightforward alcohol. A volatile, flammable, colorless liquid known as ethanol has a distinctive wine-like odor and bitter flavor. It is a psychotropic stimulant used recreationally, as well as the primary component in alcoholic beverages. Ethanol may be made naturally by yeasts fermenting carbohydrates or artificially using petrochemical processes like ethylene hydration. As an antiseptic and disinfectant, it has uses in medicine. It is employed in the synthesis of organic

	molecules as well as as a chemical solvent. Fuel is a source of ethanol. Dehydrating ethanol yields ethylene, a crucial chemical feedstock [53].
(3-Aminopropyl)triethoxysilane	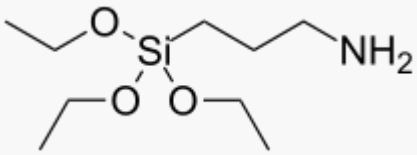 An aminosilane often employed in the silanization procedure, which involves functionalizing surfaces with alkoxysilane molecules, is 3-Aminopropyltriethoxysilane (APTES). Additionally, it may be utilized to covalently link organic films to metal oxides like titania and silica [54].
Glutaraldehyde	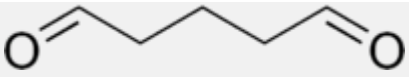 Glutaraldehyde is a disinfectant, medicine, preservative, and fixative that is marketed under the trade names Cidex and Glutaral, among others. It is used for a number of applications but most important it serves as a disinfectant and is employed in hospitals to sanitize equipment used in surgery, also used for cross-linking and as a tanning agent, as an antimicrobial in water-treatment systems and in the preparation of grafts and bioprotheses. When employed, protective equipment is advised, especially in areas with high concentrations. In addition to spores, glutaraldehyde is efficient against a variety of bacteria [55].
Collagen	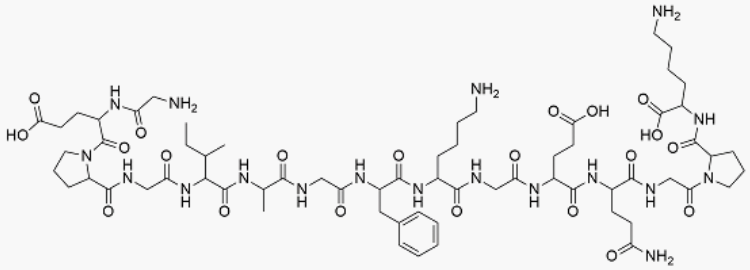 The primary structural protein in the extracellular matrix that makes up the many connective tissues of the body is collagen. It makes up between 25 and 35 percent of the protein in a mammal's whole body and is the primary building block of connective tissue. The collagen helix, a triple helix of an extended fibril made of amino acids, is what makes up collagen. It is mostly present in connective tissue, which includes skin, tendons, ligaments, cartilage, and bones [56].

3.2. Procedures

3.2.1. Fabrication of Macro-PSi samples

MacroPSi samples were fabricated by the anodic dissolution of boron-doped p<100>silicon wafers with a resistivity of 10-20 Ω-cm in HF solution. The degree of doping and the resistivity are inversely proportional, that is a heavily doped wafer will have lower resistivity. We cut 2 cm x 2 cm pieces of silicon. We applied 2 minutes of washing with 5% HF and then 3 minutes wash with Mili-Q water (Figure 10). Afterwards, we washed the sample with water and then dried I with pressurized air. Next, we put the sample inside the electrochemical cell so that the polished part of the silicon is in contact with the O-ring and the back in contact with the aluminium foil on a Cu plate (Figure 11).

To perform the anodization we used a solution of hydrofluoric acid (40%) in N, N dimethylformamide (DMF) (1:10) and applied a current density of 5 mA/cm^2 at different times(Figure 6)[57].

Once the electrochemical anodization its done, our PSi it is going to look like Figure 12.

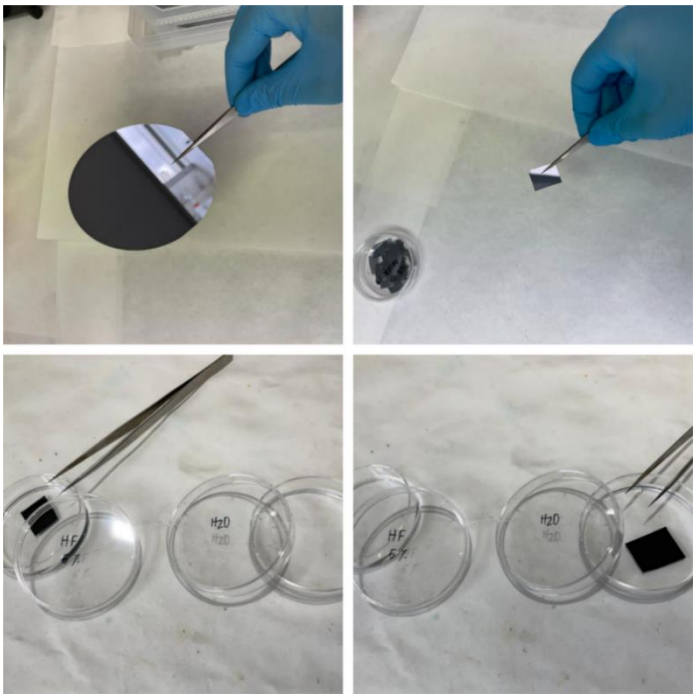

Figure 11. First steps for the electrochemical anodization

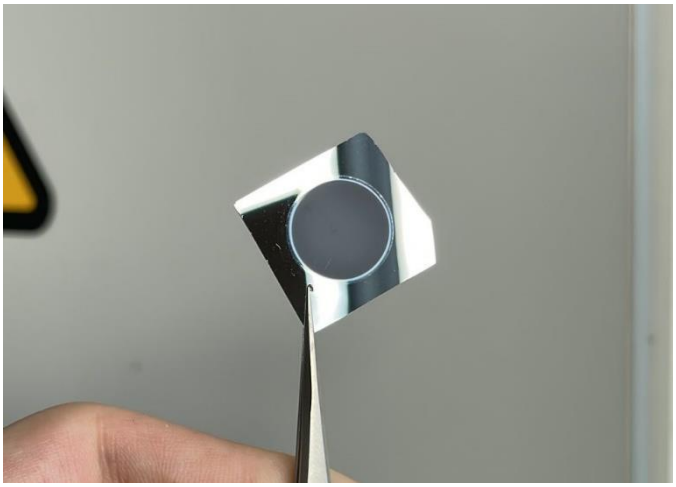

Figure 12. Results of anodization

3.2.2. Chemical modification of PSi surface

Macroporous silicon samples were modified with 1H, 1H, 2H, and 2H-Perfluorooctyltrichloro silane (FOTS) via physical vapour deposition. The PSi substrates were placed in a sealed vessel with a container filled with silane precursor liquid.

There was no direct contact between the liquid and the substrates. The vessel was 1 h under low pressure at room temperature followed by annealing at 120 ºC for 2 h in the oven. (Figure 13).

Figure 13. FOTS steps to modify PSi surface

3.2.3. Fabrication of PDMS replicas from macro-PSi

A prior study's salinization technique for PDMS was used. The silicone elastomer foundation was specifically homogeneously mixed with one part of the curing agent (SYLGARD®, Dow Corning, USA) (Figure 14), cast into individual wells, and degassed for 30 minutes to eliminate air bubbles in a vacuum chamber (we can see the before and after in Figure 15). The degassed PDMS was poured onto PSi sample and then 3 hours at 70 °C [47] (Figure 16).

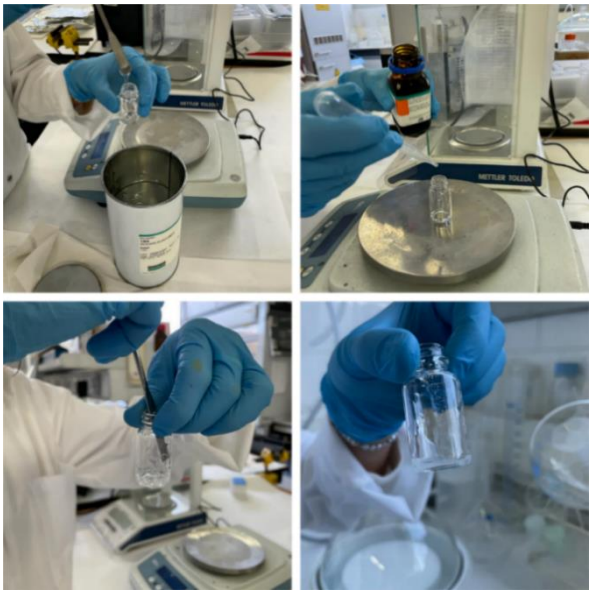

Figure 14. Steps to make the silicone elastomer

Figure 15. Before and after of degasification of PDMS

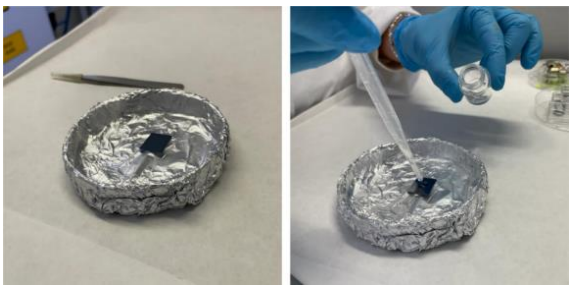

Figure 16. Applying PDMS degasified directly to the PSi

3.2.4. Fabrication of PGLA replicas from PDMS structures. Manufacture of polymeric replicas with PGLA from PSi and polymer PDMS

We started preparing a mix with PGLA and DCM. To do that we did the following calculations to achieve the perfect mix (Annex 1)

We needed 1.325 ml DCM and 0.1472 gr of PGLA (We can see in Figure 17 and Figure 18 how we are preparing and mixing the solution to get the final product, the PGLA).

Once we had the mix, we left it to the agitator for 2 hours and after that, the solution looked completely transparent and liquid.

Once it was done, we applied the solution on the PDMS replicas and with a lot of care, we added the samples in the refrigerator, and we left it 24 hours there (Figure 19). After this time, we peeled the PGLA from the PDMS (Figure 20).

Figure 17. Preparing PGLA; (1) Tiny container where we are going to prepare our mixture; (2) and (3) measuring quantity of PGLA needed

Figure 18. Getting the DCM to mix it with the PGLA

Figure 19. Leaving overnight the PGLA

Later, we found in another study that they were leaving the samples in the refrigerator for 48 hours instead of 24h so we tried that method too.

Figure 20. Results for PGLA

3.2.5. Functionalization of PDMS structures

To improve the surface compatibility of the substrates for cell culture, all the samples were chemically modified with protein via the covalent-binding method.

PDMS surfaces were treated with plasma oxygen for 30 sec at 50 mT and 35 sccm flow of oxygen in a plasma chamber and incubated with 10% APTES in ethanol for 1 h at room temperature under nitrogen. The PDMS sample was washed twice with ethanol and distilled water and 1h at 100 ºC. Following that, the APTES-PDMS was incubated with 2.5% GTA solution in ethanol for 1 h at room temperature, and then washed twice with ethanol and distilled water. Then, the sample was immersed in 0.1 mg/ml of Collagen Type I in 0.1 M acètic acid and stored at 4 ºC overnight before washing twice with distilled water.

Figure 21. Materials used for the functionalization of PDMS structures

Figure 22. Final steps for the functionalization of PDMS

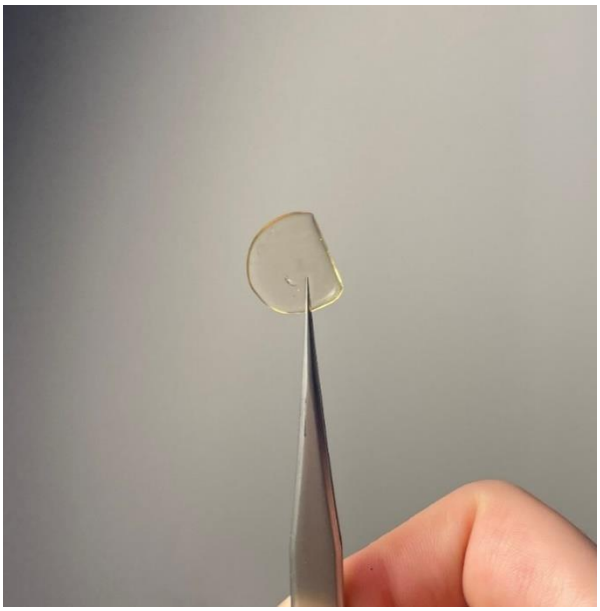

Figure 23. Final result of functionalization of the PDMS

4. Results and discussion

An increasing amount of attention has been paid in recent years to studying cell surface interactions, particularly in the field of biomaterial research for medicines, diagnostics, and regenerative medicine. To determine the ideal circumstances for cell adhesion, growth, and proliferation, it is essential to investigate the impact of surface chemical changes on cellular activity. Understanding how cell-surface interactions and surface functions affect cell anchoring on chemically changed substrates is essential for this [58].

4.1. Fabrication and characterization of Macro-PSi

P-type silicon was utilized to create disordered macroporous silicon, which was then employed as a template. Macroporous silicon was created using a silicon wafer that was etched at J=5 mA/cm^2 and ρ=10-20 Ωcm for 10 minutes on sample A, at J=5 mA/cm^2 and ρ=10-20 Ωcm for 15 minutes on sample B, at J=5 mA/cm^2 and ρ=10-20 Ωcm for 15 minutes on sample C, at J=5 mA/cm^2 and ρ=10-20 Ωcm for 20 minutes on sample D and at J=5 mA/cm^2 and ρ=10-20 Ωcm for 20 minutes on sample E.

Figure 24 shows SEM images of a top and cross-section view of microporous silicon substrates.

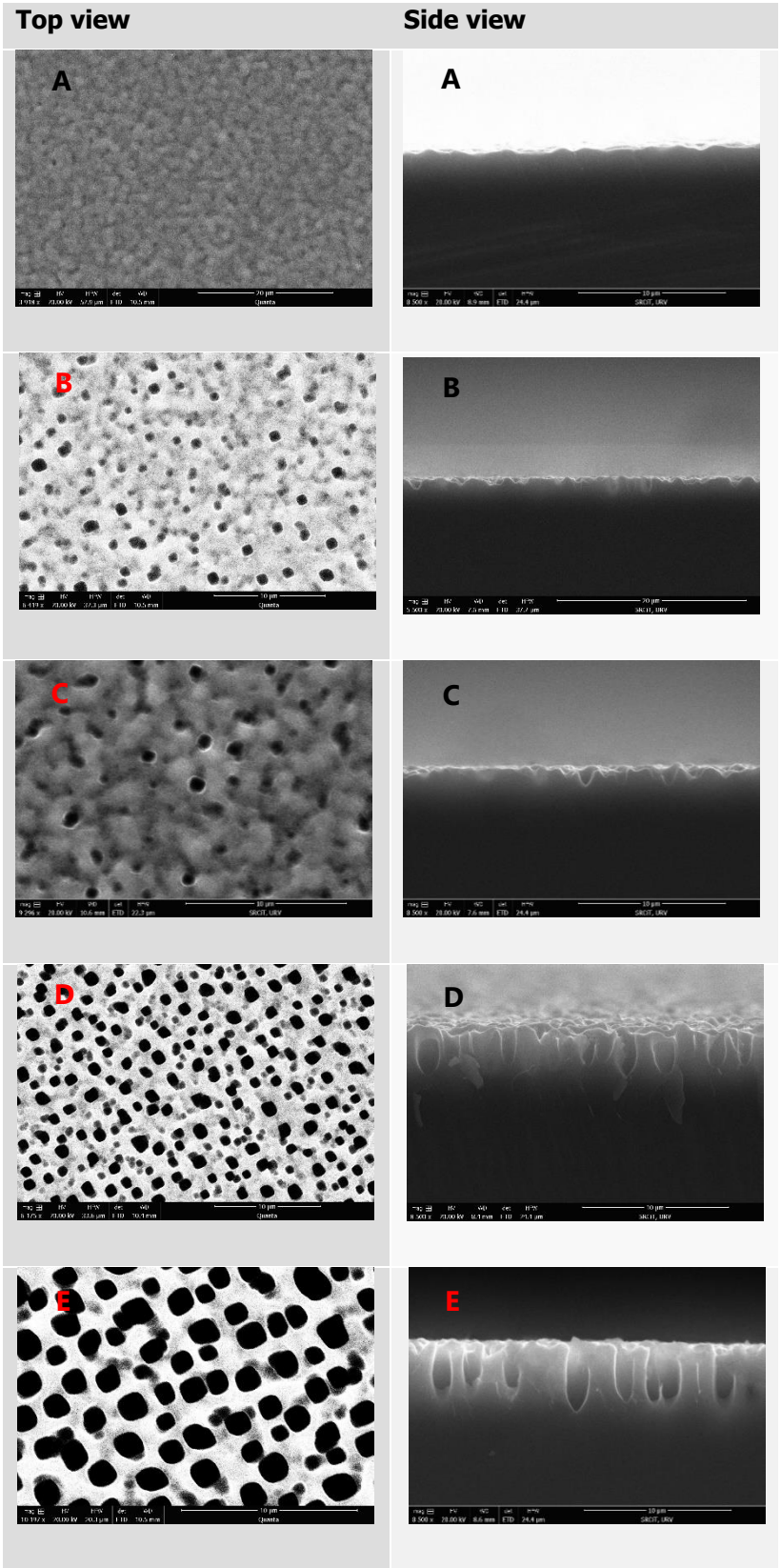

Figure 24. SEM images of Top and side view of PSi

Right after we took those pictures with the SEM, we decided to measure the porosity of each one using ImageJ program.

With ImageJ we could study the porosity of the SEM pictures by opening any image we wanted to use for the porosity measurement, cropping with the rectangular selection tool the largest rectangular section of the coating without including the interface and using the thresholding tool to select the area of porosity.

After that, we got the results we can see in Table 8. Last column it is the most important one since it is the column that it is going to explain us the porosity in each sample.

Table 8. Characteristics of Porosity in samples A,B,C,D,E

Sample name	Count	Total Area	Average Size	%Area
A	6767	2.628	3.882E-4	0.531
B	6851	19.077	0.003	3.608
C	6479	13.037	0.002	2.608
D	9518	140.433	0.015	28.045
E	8020	228.008	0.028	45.461

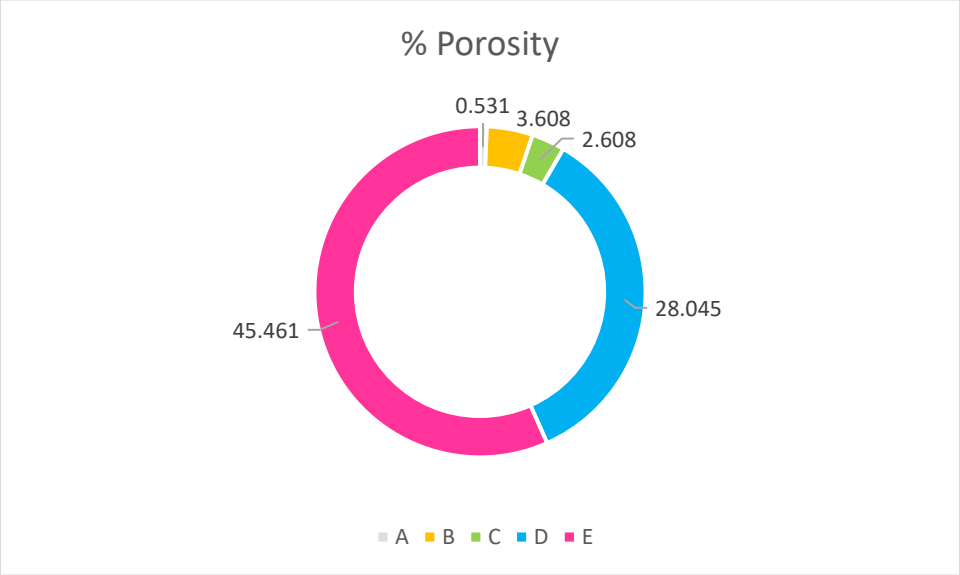

Figure 25. Chart showing off the porosity comparison from table 8

We can compare the different porosities in the chart shown in Figure 25. As expected just by looking at the SEM pictures, we got the next results (from highest porosity to lowest):

Sample E > Sample D > Sample B > Sample C > Sample A

Table 9. Geometrical parameters and contact angle values of MacroPSi substrates

Sample name	Time (minutes)	Pore length (µm)	Porosity (%)	Contact Angle (º)	Standard deviation	Error
A	10	No pores	0.531	73.942	0.232	0.021
B	15	1.130	3.608	80.793	0.201	0.018
C	15	1.840-2.360	2.608	84.628	0.819	0.078
D	20	2.500-2.890	28.045	86.174	0.227	0.031
E	20	3.900-4.630	45.461	93.547	0.683	0.062

We can observe in Table 9 that the increase in porosity is proportional to the increase in the length of the pore.
Therefore, when porosity increases, the contact angle value also increases, making the most porous surfaces end up being the most hydrophobic.

Also, we can see there's a direct relation between time, pore length and contact angle. The longer we leave the sample to anodize, the longer the pores get and the higher the contact angle is.

+ Time = + Pore length = + Contact Angle value

After seeing these preliminary results from the first group of samples (A, B, C, D, E), we decided to make samples that have smaller wells (pore length needs to have a range from 0.5 to 2 µm aproximately) because we want to replicate the mirrored surface with PDMS which has a high degree of softness.
If the pore length surpasses that range, we are going to face that the pillars from the same replica are going to be completely different (too high) from other replicas due to the softness characteristics of the PDMS polymer .

So, we decided to fabricate another serie of samples (X, Y, Z). The anodization conditions for these samples were the following:

Sample X: J=4 mA/cm^2, t=10 minutes, HF:DMF (1:10)

Sample Y: J=5 mA/cm^2, t=8 minutes, HF:DMF (1:10)

Sample Z: J=6 mA/cm^2, t=6 minutes, HF:DMF (1:10)

Table 10 shows the geometrical parametres of these macroPSi substrates.

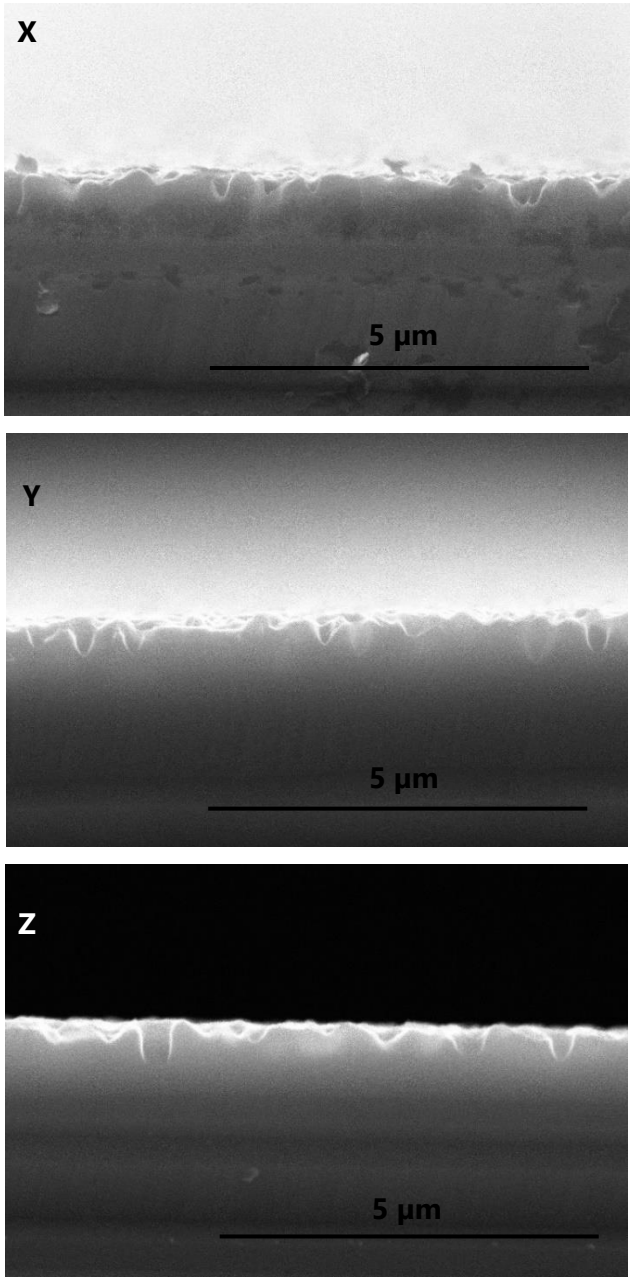

Figure 26. PSi side view of samples X,Y and Z

Table 10. Characteristics of samples X,Y,Z

Name sample	Pore length (µm)	Porosity (%)	Contact Angle (º)	Standard deviation	Error
X	0.995	3.201	90.820	0.142	0.012
Y	1.315	3.623	97.820	0.613	0.052
Z	0.743	2.857	84.700	0.372	0.034

As we can see in Table 10 and the images from figure 26, our pore length goes from 0.5 µm to almost 1.5 µm, numbers that are within the range we were seeking.

Now, if we pay attention to the samples, we can tell that there's a direct relation between the contact angle and the pore length; Also, with these results, we can even see more clearer that the porosity it also has a direct relation with pore length and contact angle, leaving the scheme like the following:

+ Pore length = + Contact Angle value = + Porosity

4.2. Chemical modification and wettability properties of the Macro-PSi substrate.

Chemical modification of silicon substrates offers a solution for the production of hydrophobic surfaces. In this work, PSi surfaces were modified using a hydrophobic surface coupling agent (FOTS) in order to increase the hydrophobic properties of the material. The surface property of the Psi-FOTS was characterized and the contact angle with water was analyzed.

As I explained before, we measured the water contact angle using a Theta Optical Tensiometer, and the hydrophobicity of each PSi, surface was assessed (Attension, Finland). A static sessile drop tangent technique was used with the Drop Shape Analysis program to determine the contact angles when a 10 µl water droplet came into contact with the surfaces. As the angle created between the substrate surface and the tangent to the drop surface, the contact angle was described.

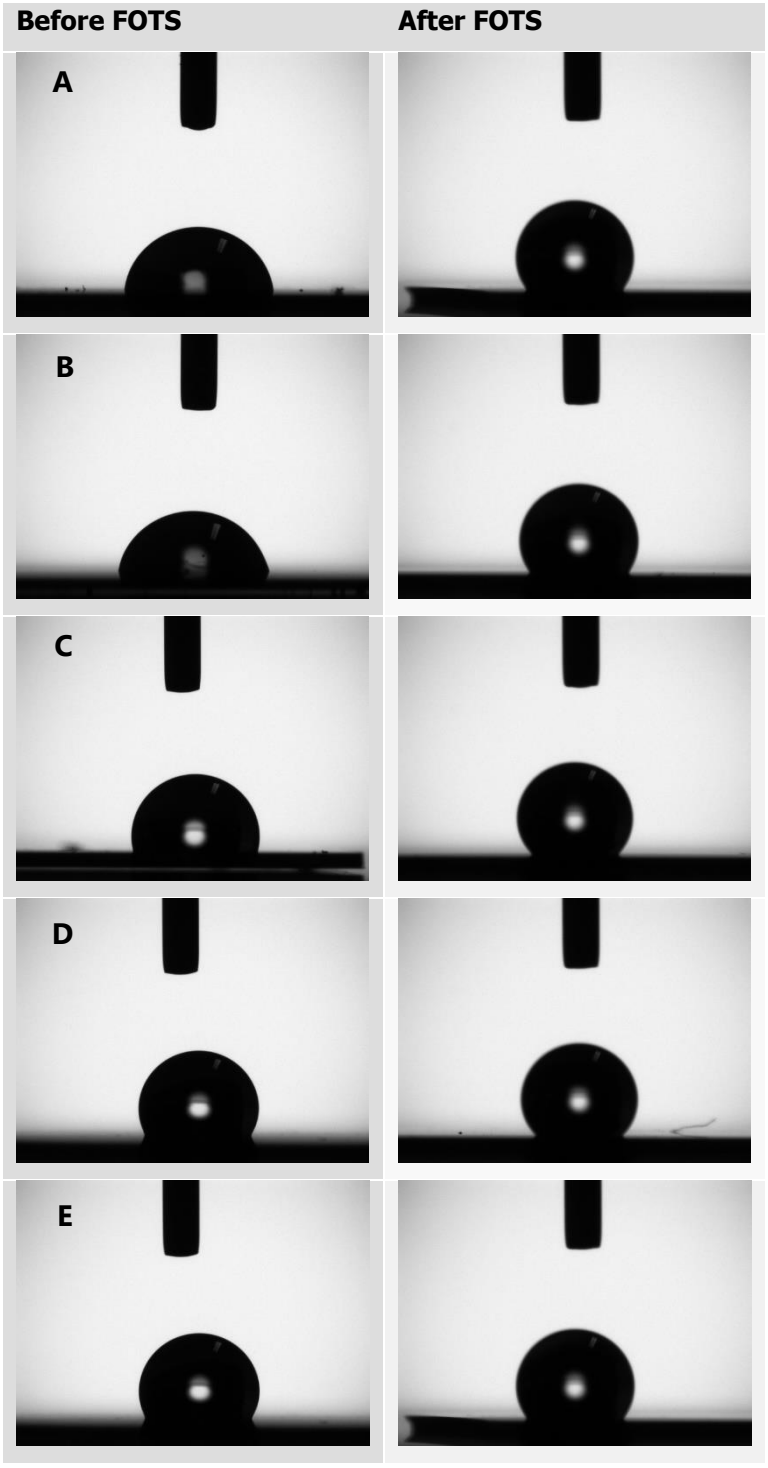

Figure 27. Before and after FOTS

Table 11. Contact angle values before and after chemical modification with FOTS

Sample name	Time (minutes)	Pore length (µm)	CA(º) before	CA(º) after
A	10	No pores	73.942	106.920
B	15	1.130	80.793	127.710
C	15	1.840-2.360	84.628	129.540
D	20	2.500-2.890	86.174	135.690
E	20	3.900-4.630	93.547	139.610

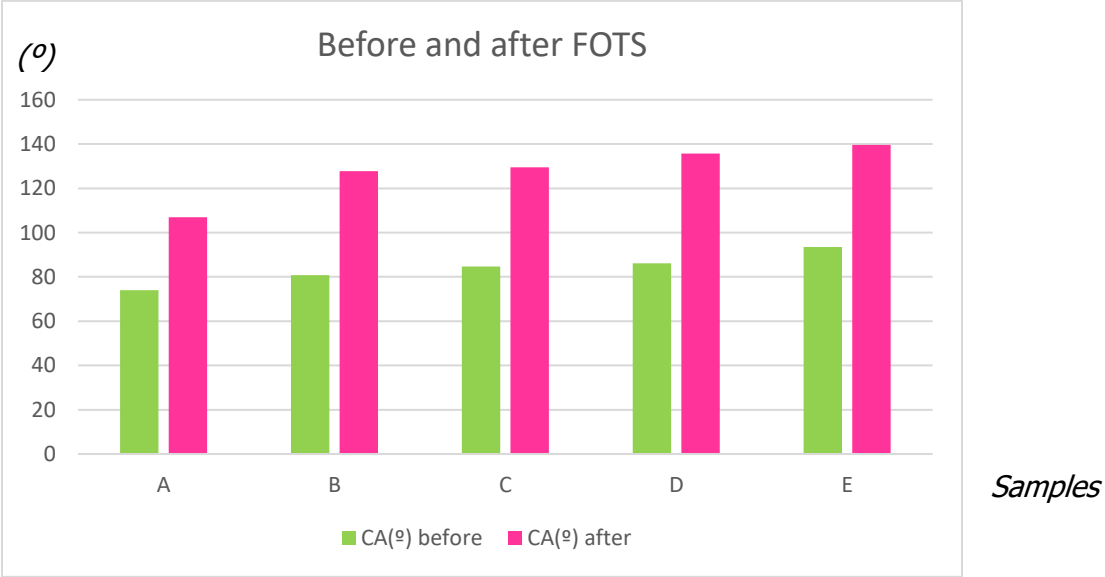

Figure 28. Before and after FOTS graphic

If we observe the tables and the graph, we can confirm that the chemical modification method has worked, since the surface has become more hydrophobic than before applying the FOTS (it is observed that the degrees of tension of the drop are greater than before). After chemical modification with FOTS, all the contact angle values increased, as we expected.

This will help us so that when we want to make PDMS replicas, they will come off more easily.

Immeditely afterwards, we proceed by applying FOTS to the rest of the samples (X,Y,Z):

Table 12. Contact angle values before and after chemical modification with FOTS

Name sample	Pore length (µm)	CA(º) before	CA(º) after
X	0.995	84.700	101.100
Y	1.315	90.820	103
Z	0.743	93.870	110

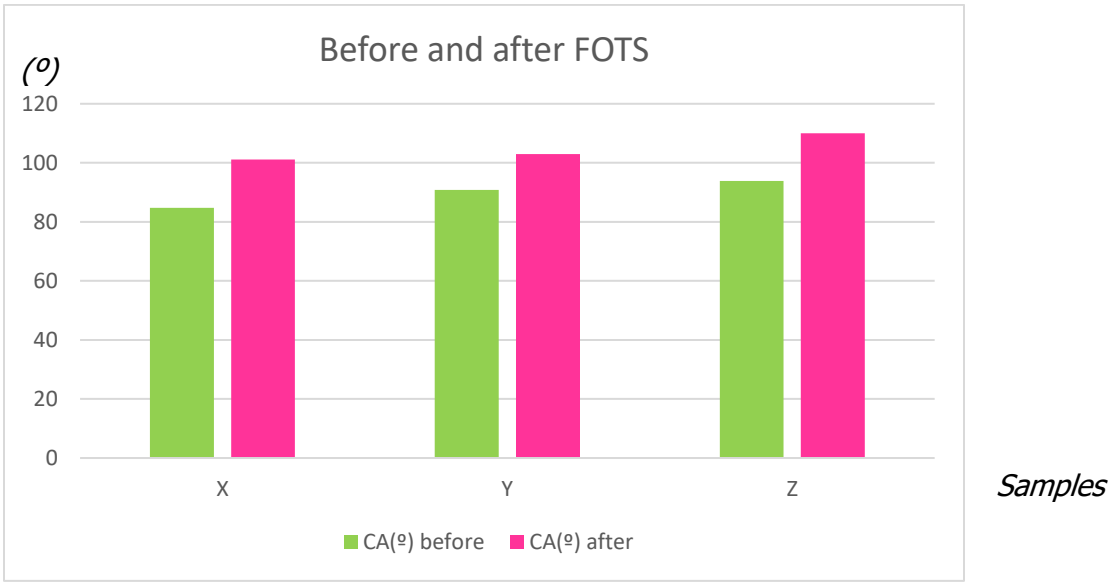

Figure 29. Before and after FOTS graphic

If we observe the Table 12 and in Figure 29, we can say that the FOTS method has worked once again, since the surface has become more hydrophobic than before applying the FOTS (it is observed that the degrees of tension of the drop are greater than before).

4.3. Fabrication of PDMS replicas

Macro-PSi-FOTS substrates were employed as template to obtain PDMS replicas. Using this method, it's not going to be necessary to dilute the polymer in a solvent because it will be cured after the infiltration procedure.

PSi samples were infiltrated using a wetting-based technique to produce the solid state of PDMS, which has to be cured at 70ºC.

In order to make the PDMS, a 10:1 mixture of liquid silicon base and a curing agent was thoroughly mixed together. The last mixture was used to cover the template and was applied at room temperature before curing for three hours at 70 ºC [47].

The final PDMS replicas obtained are shown in Figures 30, 31, 32 and 33.

ESEM pictures were taken from top side view and diagonal view of every PDMS sample (A,C,B,D,E group and X,Y,Z group).

We observe that in samples A, B and C hardly any pillars are seen and on the other hand, in images D and E many pillars can be observed.

In samples D and E, the pillars observed in their surface have all sizes and they are completely disordered, therefore, replicas could not be made with these samples since they would all come out different. This can be explained by the same PDMS propierties, it makes the pillars to bend to every single direction and making the samples very nonhomogeneous (seen in Figure 30, 31 and 32).

We also applied the PDMS on X, Y and Z samples and we can observe that, the formed pillars are very similar to each other, making the sample more homogeneous (seen in Figure 33) than the samples from the first group (A, B, C, D, E samples).

We can say, therefore, that the 'well' range that we had mentioned (0.5 to 2 μm) is a good option for the objectives we have set ourselves.

PDMS top view

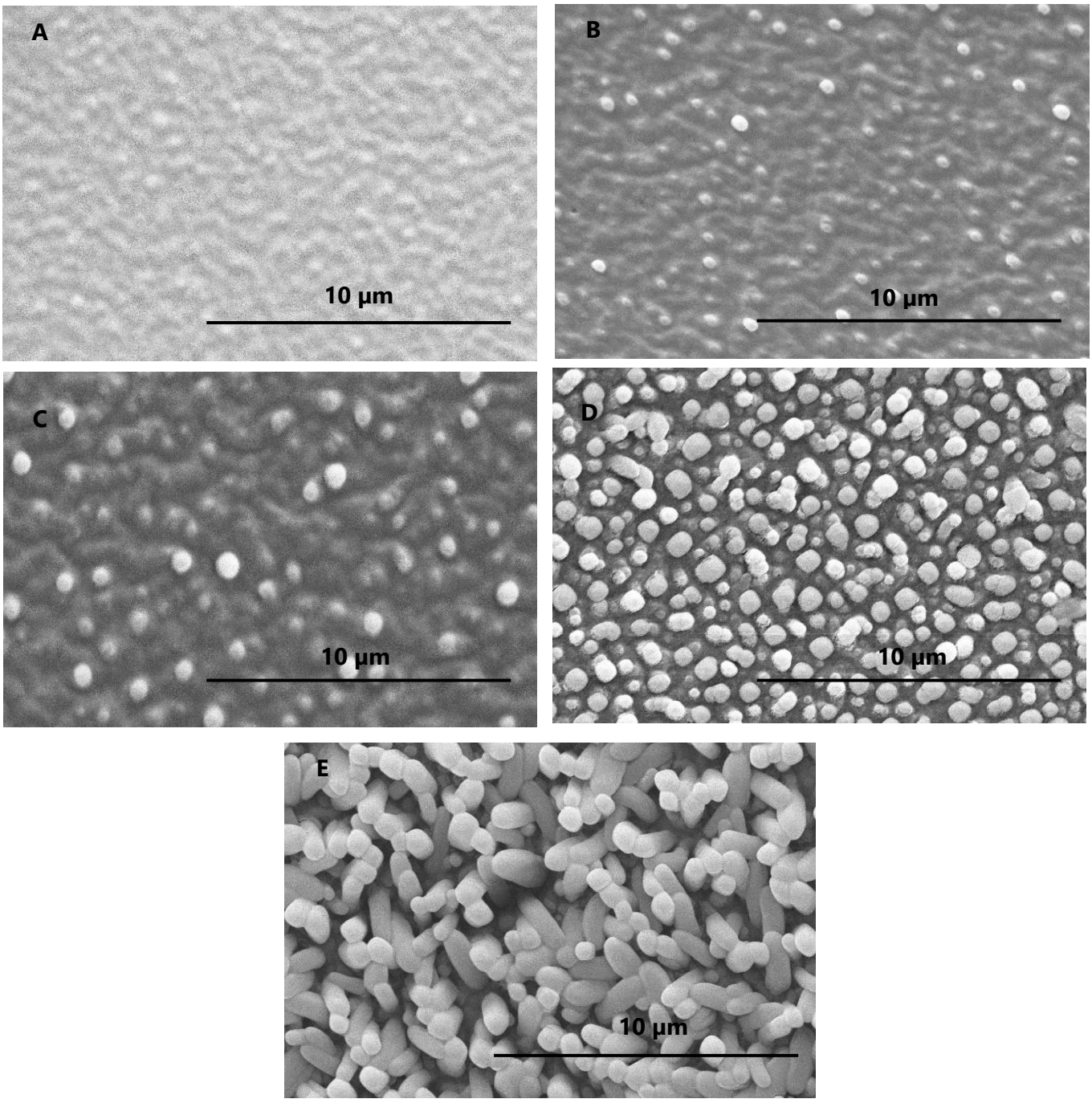

Figure 30. PDMS top view replicas for the A, B, C, D, E samples

PDMS diagonal view

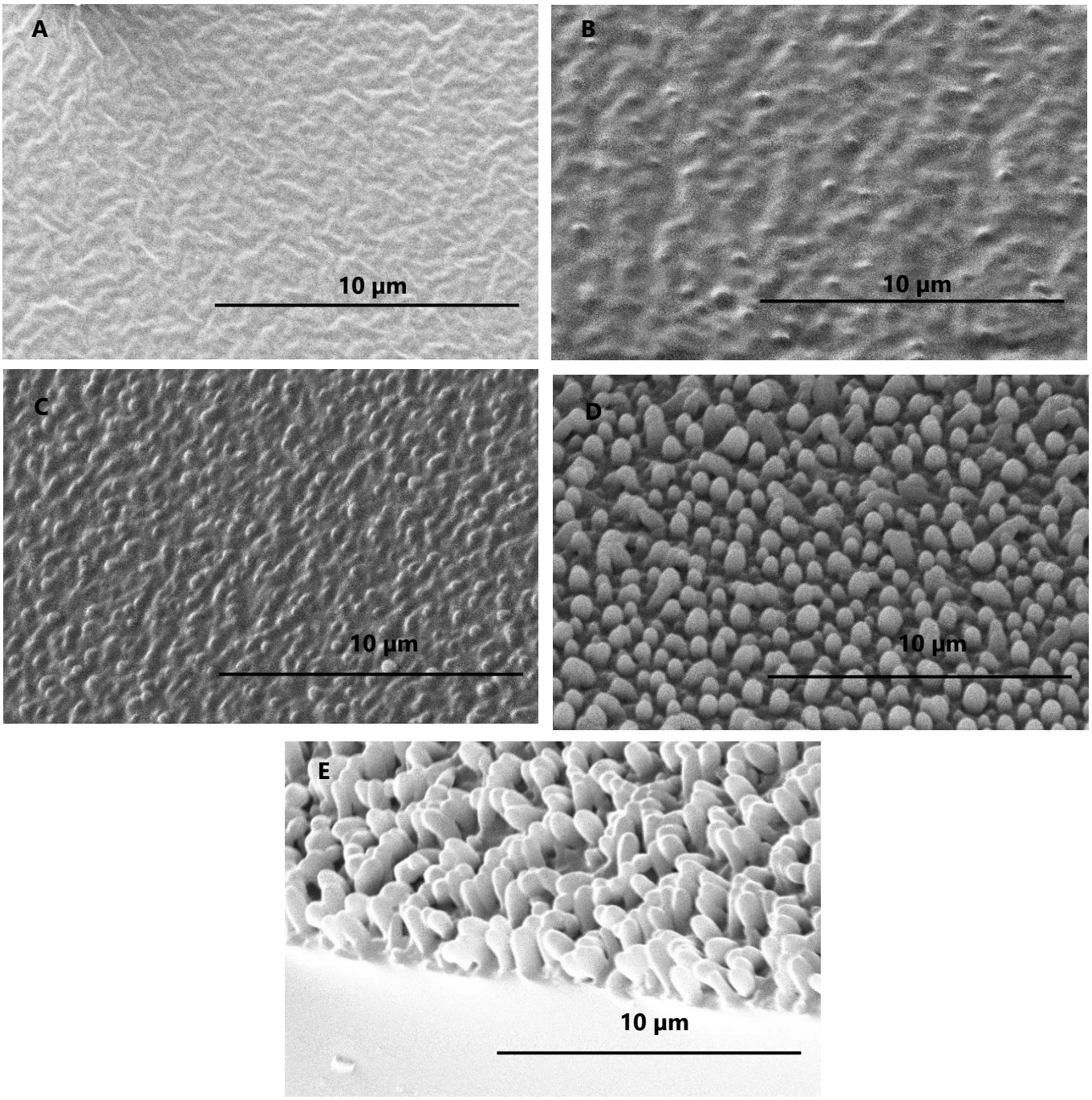

Figure 31. PDMS diagonal view replicas for the A, B, C, D, E samples

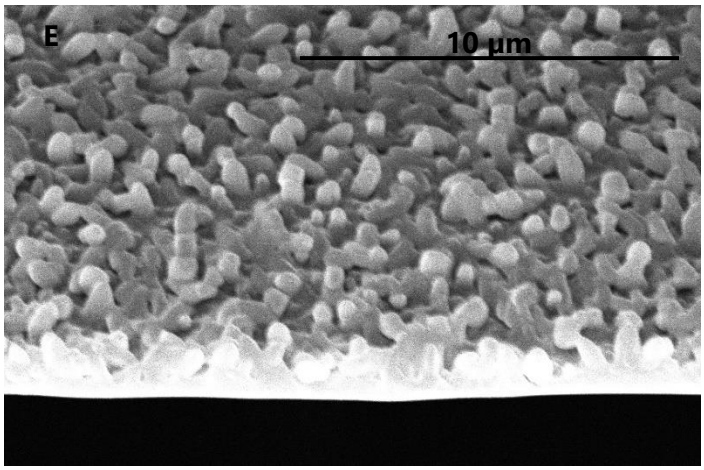

Figure 32. Nonhomogeneous PDMS surface from sample E

PSi-PDMS top view

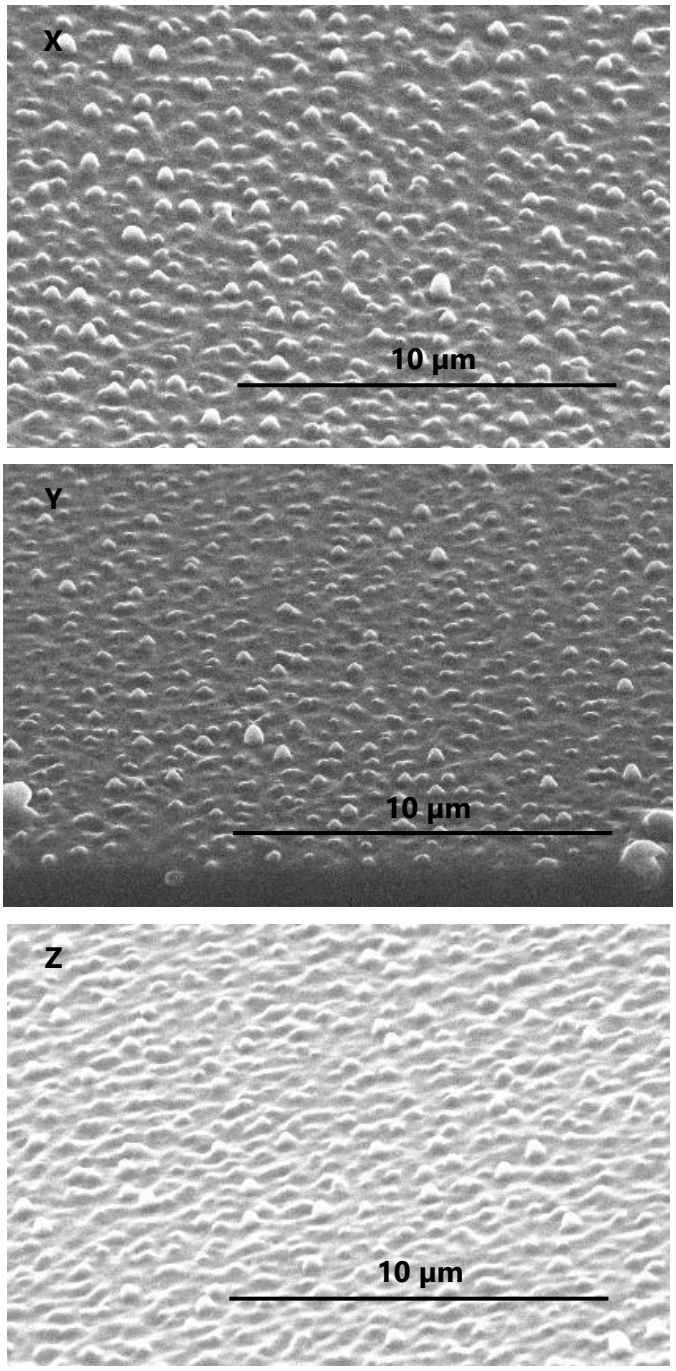

Figure 33. Top view PDMS of samples X,Y and Z

4.4. Fabrication of PGLA surfaces from PDMS structures

The field of pharmaceutical and biological science has been completely transformed by PLGA, one of the most effectively created biodegradable polymers. Drug targeting and increased bioavailability have been made possible by PLGA-based formulations, whose physicochemical characteristics of PLGA have a significant impact on drug release and degradation [61].
When PGLA is cured, the result achieves a solid surface, whereas the PDMS resembled a gelatin, making the results of PDMS softer. Since its consistency/characteristics are very different from the PDMS, we had to try to make replicas of PGLA, but instead of using PSi as a mold (like we used to make the PDMS replicas), we used the PDMS replicas as a molds, that way, we can make mirrored replicas of PGLA (pores/wells instead of pillars).

In order to create the solid state of PGLA, we had to mix DCM with PGLA using some calculus (shown in Annex 1- Figure 42) and cured overnight at the refrigerator (24h and 48h).

We did two batches of X, Y and Z samples; the first batch was left overnight for 24 hours, and the second batch was left in the refrigerator for 48h, so we could observe if it makes much of a difference leaving the PGLA curing more time.
Figure 34 are the samples of PGLA that were left overnight for 24h in the refrigerator and Figure 35 are the samples of PGLA that were left in the refrigerator for 48h.

As we can see in Figure 34.(X) the pores look very well done and overall, the sample looks very homogenic, whereas, in Figure 34.(Y and Z) pores are not that well done but there's still made and it doesn't have as much porosity as in sample X.
On the other hand, in Figure 35.(X) the pores still look very well done but the porosity is not as high as in the 24h curing sample X (Figure 34.(X)), whereas, in Figure 35.(Y and Z) there are no pores but the surface is seemingly wrinkled, as if the pores where about to be created but it never quite happened.

PDMS-PGLA top view

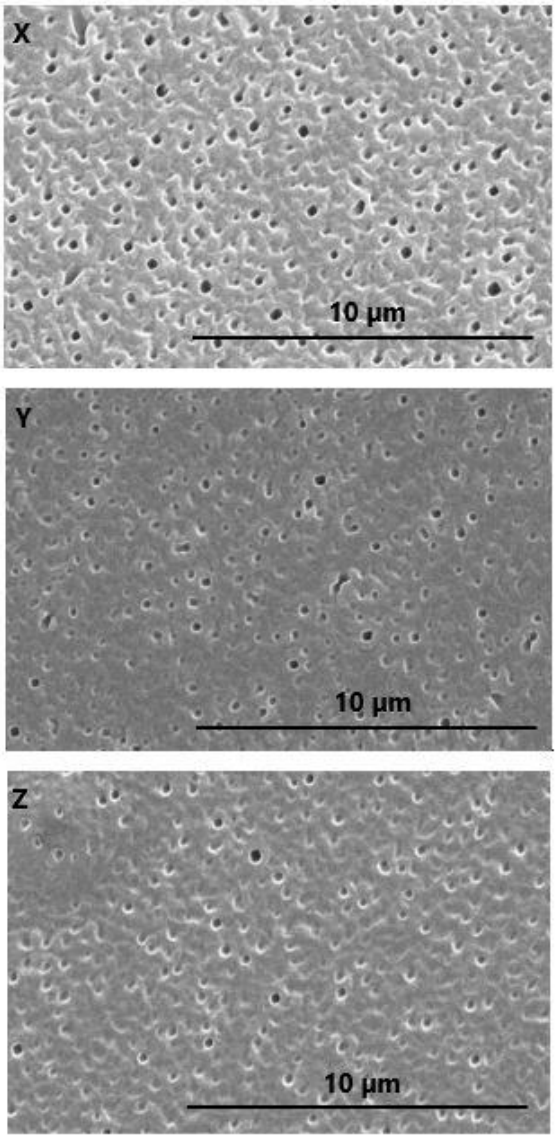

Figure 35. PGLA cured overnight 24h

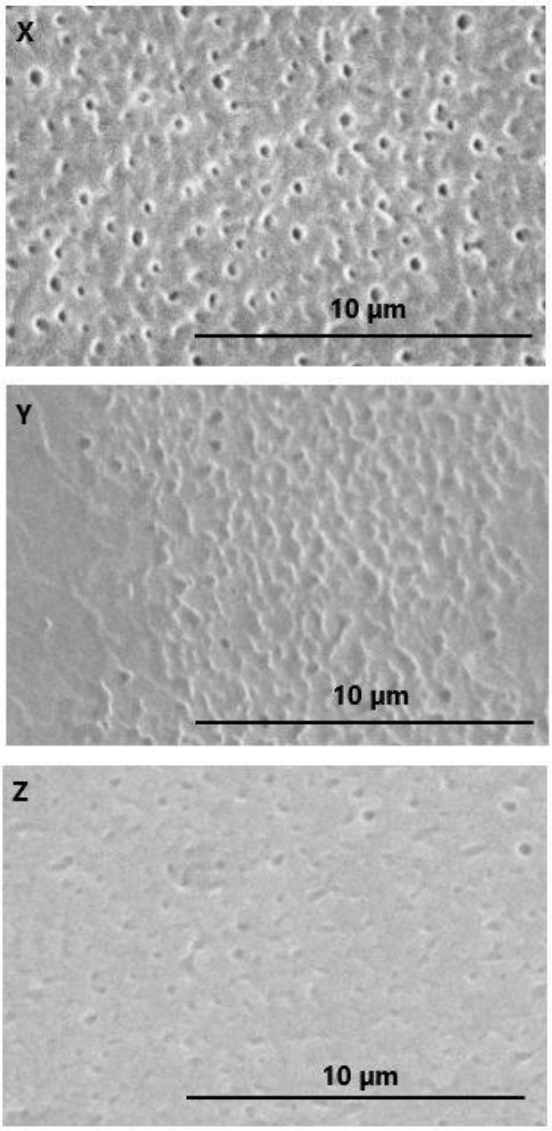

Figure 34. PGLA cured 48h in the refrigerator

So, in conclusion, we can clearly say that the 24h curing is much better step than the 48h curing.

4.5. Functionalization of PDMS structures

Due to its low cost, straightforward and quick construction process, and optical transparency, polydimethylsiloxane (PDMS) is widely employed, even though, the low surface energy of PDMS makes it difficult to attach to many substrates [62]. So, in order to achieve the attachment of cells to the PDMS, we had to apply a functionalization so that such binding would occur.

PDMS surfaces were being exposed to plasma oxygen for 30 seconds at 50 mT and 35 sccm of oxygen flow in a plasma chamber, and then those were incubated with 10% APTES in ethanol for an hour at ambient temperature under nitrogen, as we described in the procedures.

The PDMS sample was twice cleaned in ethanol and distilled water and then heated to 100 ºC for one hour. The APTES-PDMS was then cleaned twice with ethanol and distilled water before being incubated for 1 hour at room temperature with a 2.5% GTA solution in ethanol. The sample was then dissolved in 0.1 mg/ml of collagen type I in 0.1 M acetic acid, kept at 4 ºC for an overnight period, and then washed twice with distilled water.

As we can see in Figure 36, after the PDMS surface got exposed to the plasma oxygen, radicals of OH are left in that same surface. Then, the APTES is applied, it creates an easy bonding between the OH radicals and the molecule of the APTES leaving a silanized PDMS surface.
After that step, Glutaraldehyde (GTA) is applied to the silanized PDMS surface, getting attached to it, making the next step (which is adding the Collagen type I to the PDMS) easier to stick to that surface.

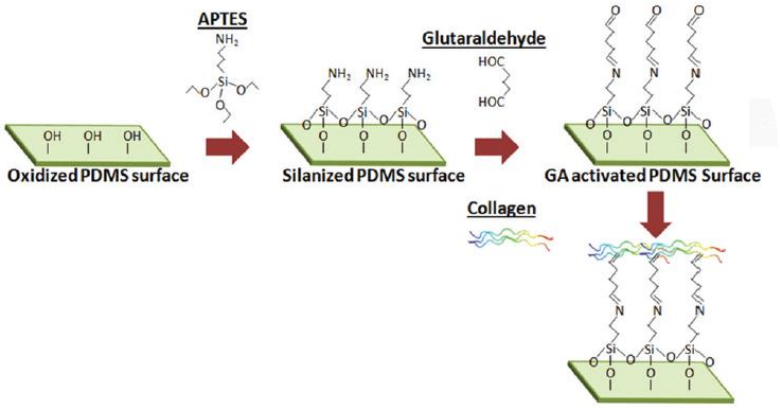

Figure 36. Scheme of the step-by-step functionalization of PDMS structures [47].

Sample X, before applying the plasma, had a mean of the contact angle of 88.32º (Figure 37); right after applying the plasma, the contact angle decreased to 47º (Figure 38).

That means that the plasma step was well done [48] as we can see in Figure 44 (annex), so we could proceed to the next step.

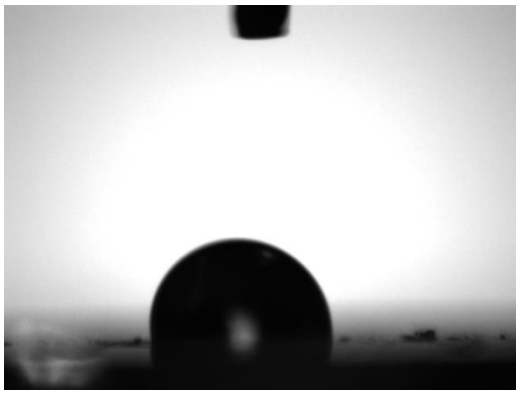

Figure 37. Contact angle before plasma step

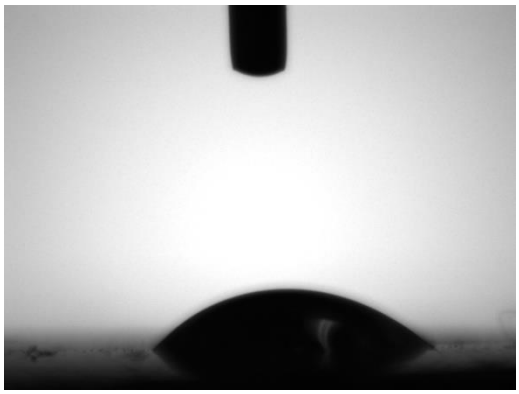

Figure 38. Contact angle after plasma step

After the plasma step, right after the salinization with ethanol + APTES happened, we had a 74.200º contact angle (Figure 39).

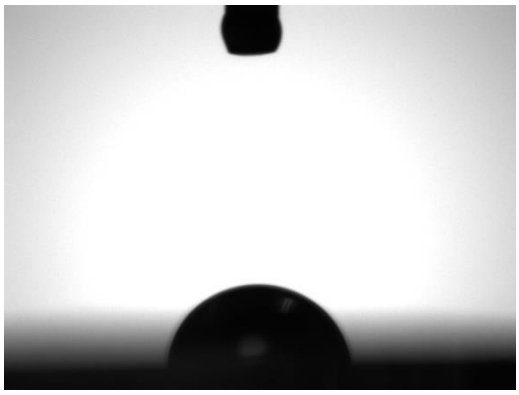

Figure 39. Contact angle after APTES

And finally, when we applied our collagen to our sample, we could see that the contact angle went from 74.200º to 81.100º (Figure 40). The functionalization worked. We can see every step and its contact angle in Table 13.

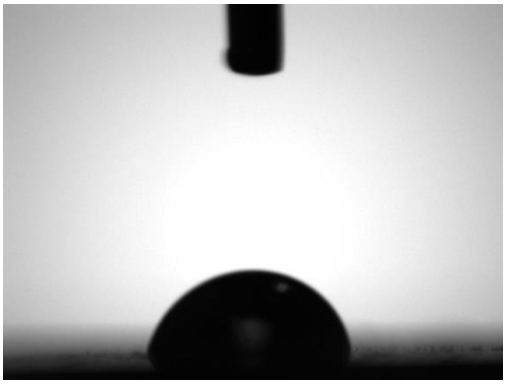

Figure 40. Contact angle after Collagen

Table 13. Contact angle on every step on the Functionalization of PDMS structures

Functionalization of PDMS structures steps	Contact angle
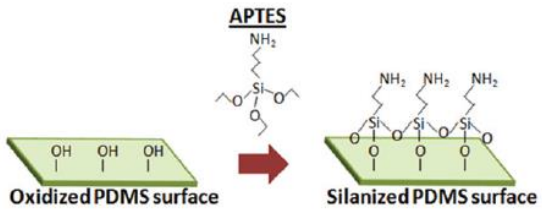	88.320º 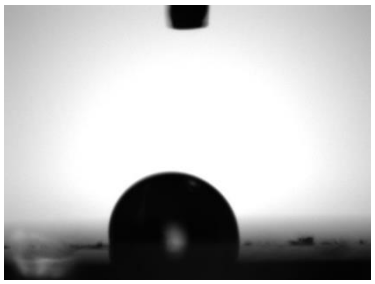
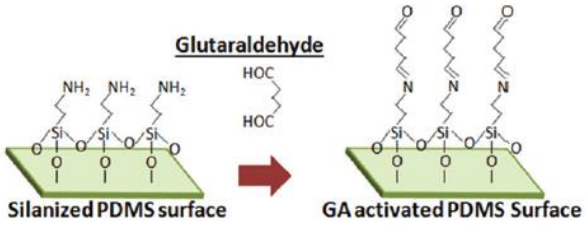	47º 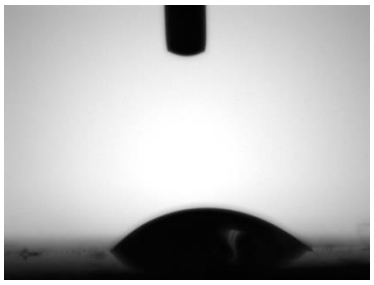
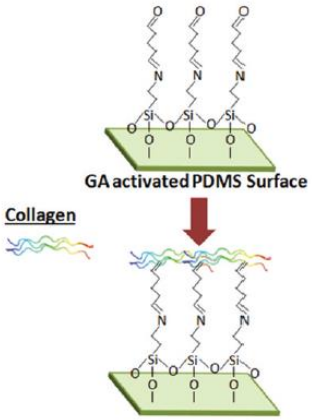	74.200º to 81.100º 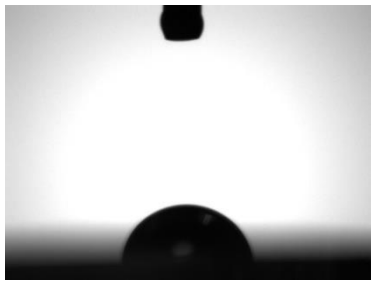 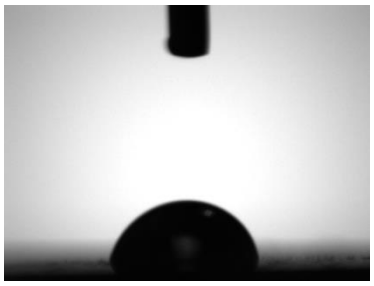

So, as a summary, APTES/ethanol + GTA were used in this investigation to silanize the PDMS surface before the Collagen type I immobilization. According to the water contact angle, the natural PDMS surface was hydrophobic (within the range that goes from 85º to 100º), indicating that it was not water-wettable (or hidrophobic). The surface of PDMS + Collagen type I was still

hydrophobic (81.100º) despite Collagen type I adsorption having a somewhat smaller impact on the contact angle.

This investigation revealed that PDMS silanization by APTES with GTA may decrease the contact angle to the hydrophilic zone (<60°), which is known to dramatically lower the hydrophobicity of the PDMS surface. The contact angle was further decreased (by around <50°) as a result of Collagen type 1 protein adsorption on these chemically altered surfaces which meant that the functionalization was well done and after that we could proceed to the next step, cell adhesion and the differentiation on protein layer.

So, with those results we can say that a hydrophilic surface with functional groups is present on chemically altered PDMS surfaces with APTES/ethanol+ GTA + Collagen type I, facilitating improved attachment of the Collagen type 1 protein. Increased Collagen type 1 immobilization on APTES-GTA modified PDMS surfaces may improve osteogenic differentiation because Collagen type 1 encourages cell proliferation [47].

4.6. Other forms

As a plus, we decided to take the experimentation further away and we decided to try to make PDMS replicas out of different Macro-PSi forms such as pyramids and lines (Figure 41 and 42). The molds were already fabricated by lithography, so we proceeded to apply the PDMS on those surfaces to see the different patterns.

4.6.1. Pyramids

When we can see in Figure 42, that the pyramids did not quite form completely due to the characteristics of PDMS (most likely its density), so, instead of looking like a well-formed pyramid, it looks like a pyramid without the tip on the top.

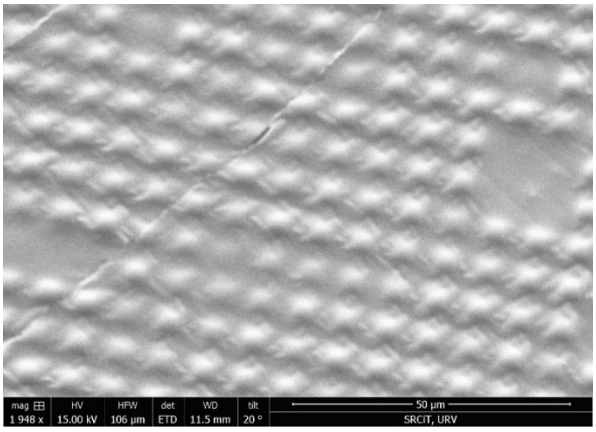

Figure 41. Pyramids made of PDMS from top side view

4.6.2. Lines

As we can see in Figure 43, the lines are well formed but if we take a closer look, the edges are not completely straight, they are rather round-ish, that's due to (again) the characteristics of PDMS (most likely its density).

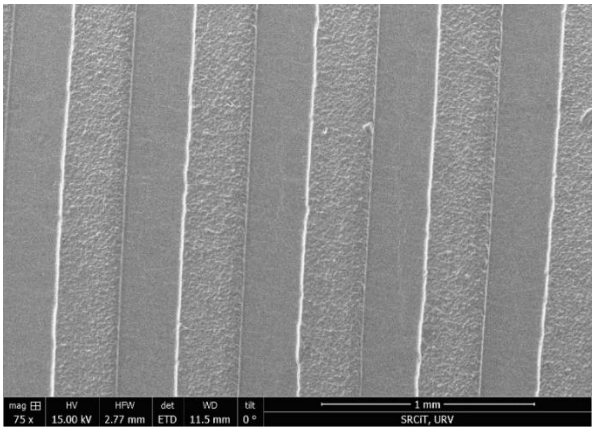

Figure 42. Lines made of PDMS from top side view

Conclusions and future directions

From the discussed results in the previous section, we can extract the following conclusions:

1. We created PSi out of p-type silicon wafers which we used later on as templates to obtain replicas with polymers.

2. We have seen that there is a direct relation between pore length, contact angle and porosity for PSi, summarized in the following statement:

   The longer we leave the sample to anodize, the longer the pores get and the higher the contact angle is.

   + Time = + Pore length = + Contact Angle value

3. We used 2 types of polymers to make the replicas:
   a. PDMS: to make PDMS replicas, we used our PSi template and we stablished that its wells must oscillate between 0.5 µm to 2 µm with the aim of making homogeneous replicas due to the characteristics of PDMS (has a high degree of softness). In order to achieve that, the PSi templates had to be made with the following anodization conditions:

      Sample X: J=4 mA/cm^2, t=10 minutes, HF:DMF (1:10)
      Sample Y: J=5 mA/cm^2, t=8 minutes, HF:DMF (1:10)
      Sample Z: J=6 mA/cm^2, t=6 minutes, HF:DMF (1:10)

      We have seen that, to peel off the PDMS easily, we had to apply FOTS on the templates, since it made their surfaces more hydrophobic (as we could see in Figure 28 and Figure 29).
      PDMS was a success, its replicas were very well done, leaving sample X as the best one of the pack.

   b. PGLA: to make PGLA replicas, we used PDMS as a template instead of using the PSi. Due to the characteristics of PGLA (it is a solid polymer, not as soft as the

PDMS) the replicas we made were also a success, leaving sample X as the best one of the pack.

Plus, we have also observed that replicas of PGLA can be cured in 24h or in 48h **but** it is way better if we cure them 24 hours instead of 48 hours.

4. Working with PDMS was a bit easier than working with PGLA. PDMS, before curing, it has a very viscous density, making the application of it easier when you have to pour it on top of the template. Also, it peels off right away.

5. Even though that working with PGLA it is more difficult than working with PDMS, working with PGLA it is also quite easy, but it is definitely more delicate and challenging.
   Before curing, the PGLA is completely liquid, making the application of it when you have to pour it on top quite difficult (it is important to not spill out the polymer out of the template since after curing this becomes solid and it would be a problem for the peel off). Since both polymers are transparent, it is quite difficult to see where to peel off, but once you have it, it peels off right away.

6. Regarding the functionalization, we have been able to see that, from the passage of the plasma to the salinization, it must be done instantly, or the silicon groups themselves will not adhere well to the surface and therefore, the rest of the process will not function [49].

7. We did functionalize the surfaces to use them in future applications (cell adhesion and differentiation on protein layer).

8. For future work, it would be possible to continue with the observation of the cells after applying the functionalization step, to see how they move through the sample and thus determine the reason for their movement and survival.

References

[1] Biomaterial. Wikipedia. https://en.wikipedia.org/wiki/Biomaterial;

[2] Porous Silicon. Wikipedia. https://en.wikipedia.org/wiki/Porous_silicon#:~:text=Porous%20silicon%20was%20discovered%20by,surfaces%20of%20silicon%20and%20germanium.

[3] Karbassian, F. (2018). Porous Silicon. In (Ed.), Porosity - Process, Technologies and Applications. IntechOpen. DOI: https://doi.org/10.5772/intechopen.72910

[4] Thakur M, Issacson M, Sinsabaugh SL, Wong MS, Biswal SL. Gold-coated PSi films as anodes for lithium-ion batteries. Journal of Power Sources. 2012;205:426-432. DOI: 10.1016/j.jpowsour.2012.01.058

[5] Adachi S. PSi formation by photoetching. In: Canham L, editor. Handbook of PSi. Switzerland: Springer; 2014. pp. 67-74

[6] Dimova-Malinovska D, Sendova-Vassileva M, Tzenov N, Kamenova M. Preparation of thin PSi layers by stain etching. Thin Solid Films. 1997;297(1-2):9-12. DOI: 10.1016/S0040-6090(96)09434-5

[7] Megouda N, Hadjersi T, Piret G, Boukherroub R, Elkechai O. Au-assisted electroless etching of silicon in aqueous HF/H2O2 solution. Applied Surface Science. 2009;255(12):6210-6216. DOI: 10.1016/j.apsusc.2009.01.075

[8] Saadoun M et al. Vapour-etching-based PSi: A new approach. Thin Solid Films. 2002;405(1-2):29-34. DOI: 10.1016/S0040-6090(01)01757-6

[9] Saadoun M et al. Formation of luminescent (NH4)2SiF6 phase from vapour etching-based PSi. Applied Surface Science. 2003;210(3-4):240-248. DOI: 10.1016/S0169-4332(03)00152-1

[10] Karbassian F, Rajabali S, Chimeh A, Mohajerzadeh S, Asl-Soleimani E. Luminescent PSi prepared by reactive ion etching. Journal of Physics D: Applied Physics. 2014;47(38):385103. DOI: 10.1088/0022-3727/47/38/385103

[11] Cullis AG, Canham LT, Calcott PDJ. The structural and luminescence properties of PSi. Journal of Applied Physics. 1997;82(3):909-965. DOI: 10.1063/1.366536

[12] Ludwig MH, Hummel RE, Stora M. Luminescence of spark-processed materials. Thin Solid Films. 1995;255(1-2):103-106. DOI: 10.1016/0040-6090(94)05631-M

[13] Chang S-S, Kurokawa S, Sakai A. Luminescence properties of spark-processed Si in air, O2, and N2 with low pressure. Applied Surface Science. 2006;252(12):4048-4054. DOI: 10.1016/j.apsusc.2005.04.054

[14] Kabashin AV, Meunier M. Fabrication of photoluminescent Si-based layers by air optical breakdown near the silicon surface. Applied Surface Science. 2002;186(1-4):578-582. DOI: 10.1016/S0169-4332(01)00690-0

[15] Zhang Z et al. Scalable synthesis of interconnected PSi/carbon composites by the Rochow reaction as high-performance anodes of lithium-ion batteries. Angewandte Chemie, International Edition. 2014;53(20):5165-5169. DOI: 10.1002/anie.201310412

[16] Stepanov AL, Trifonov AA, Osin YN, Valeev VF, Nuzhdin VI. Fabrication of nanoPSi by Ag+−ion implantation. Nanoscience and Nanoengineering. 2013;1(3):134-138. DOI: 10.13189/nn.2013.010302

[17] Darby BL et al. Insights for void formation in ion-implanted Ge. Thin Solid Films. 2011;519(18):5962-5965. DOI: 10.1016/j.tsf.2011.03.040

[18] Batalov, Rafael & Valeev, V.F. & Nuzhdin, V.I. & Vorobev, Viatcheslav & Osin, Yury & Lebedev, Denis & Bukharaev, A.A. & Stepanov, Andrey. (2014). Synthesis of Porous Silicon with Silver Nanoparticles by Low–Energy Ion Implantation. Izvestiya vuzov. Materialy elektronnoi tekhniki. 17. 295-300. DOI: 10.1134/S1063739715080028.

[19] Jamei M, Karbassian F, Mohajerzadeh S, Abdi Y, Robertson MD, Yuill S. The preparation of nanocrystalline silicon by plasma-enhanced hydrogenation for the fabrication of light-emitting diodes. IEEE Electron Device Letters. 2007;28(3):207-210. DOI: 10.1109/LED.2007.891260

[20] Savin DP, Roizin YO, Demchenko DA, Mugeński E, Sokólska I. Properties of laser ablated PSi. Applied Physics Letters. 1996;69(20):3048-3050. DOI: 10.1063/1.116835

[21] Kalkan AK, Bae S, Li H, Hayes DJ, Fonash SJ. Nanocrystalline Si thin films with arrayed void-column network deposited by high density plasma. Journal of Applied Physics. 2000;88(1):555-561. DOI: 10.1063/1.373695

[22] Poxson DJ et al. High-performance antireflection coatings utilizing nanoporous layers. MRS Bulletin. 2011;36(6):434-438. DOI: 10.1557/mrs.2011.110

[23] Nakahata T, Nakajima H. Fabrication of lotus-type porous silicon by unidirectional solidification in hydrogen. Materials Science and Engineering A. 2004;384(1-2):373-376. DOI: 10.1016/j.msea.2004.07.004

[24] Nakahata T, Nakajima H. Fabrication of lotus-type PSi by unidirectional solidification in hydrogen. Materials Science and Engineering A. 2004;384(1-2):373-376. DOI: 10.1016/j.msea.2004.07.004

[25] Bao Z et al. Chemical reduction of three-dimensional silica micro-assemblies into microporous silicon replicas. Nature. 2007;446(7132):172-175. DOI: 10.1038/nature05570

[26] Canham L. Porous silicon formation by porous silica reduction. In: Canham L, editor. Handbook of Porous Silicon. Switzerland: Springer; 2014. pp. 85-92

[27] Fukutani K, Tanji K, Motoi T, Den T. Ultrahigh pore density nanoporous films produced by the phase separation of eutectic Al–Si for template-assisted growth of nanowire arrays. Advanced Materials. 2004;16(16):1456-1460. DOI: 10.1002/adma.200400268

[28] Voigt F, Brüggemann R, Unold T, Huisken F, Bauer GH. Porous thin films grown from size-selected silicon nanocrystals. Materials Science and Engineering: C. 2005;25(5-8):584-589. DOI: 10.1016/j.msec.2005.06.035

[29] Huisken F, Hofmeister H, Kohn B, Laguna MA, Paillard V. Laser production and deposition of light-emitting silicon nanoparticles. Applied Surface Science. 2000;154-155:305-313. DOI: 10.1016/S0169-4332(99)00476-6

[30] Krishnamurthy A, Rasmussen DH, Suni II. Galvanic deposition of Nanoporous Si onto 6061 Al alloy from aqueous HF. Journal of the Electrochemical Society. 2011;158(2):D68-D71. DOI: 10.1149/1.3521290

[31] Möller H-J, Welsch G. Sintering of ultrafine silicon powder. Journal of the American Ceramic Society. 1985;68(6):320-325. DOI: 10.1111/j.1151-2916.1985.tb15233.x

[32] JakubowiczJ. Porous silicon formation by mechanical means. In: Canham L, editor. Handbook of Porous Silicon. Switzerland: Springer; 2014. pp. 93-102

[33] Striemer CC, Gaborski TR, McGrath JL, Fauchet PM. Charge- and size-based separation of macromolecules using ultrathin silicon membranes. Nature. 2007;445(7129):749-753. DOI: 10.1038/nature05532

[34] Huang X, Gonzalez-Rodriguez R, Rich R, Gryczynski Z, Coffer JL. Fabrication and size dependent properties of PSi nanotube arrays. Chemical Communications. 2013;49(51):5760-5762. DOI: 10.1039/c3cc41913d

[35] Design, fabrication, and characterization of porous silicon multilayer optical devices. Elisabet Xifré Pérez. https://www.tesisenred.net/bitstream/handle/10803/8458/Cap2Fundamentals2.pdf?sequence=3&isAllowed=y

[36] Fabrication and characterization of polymer micro- and nanostructures by template-based method. Raquel Palacios Higueras.

[37] Optpelectronic Research Center. Academia.edu. https://www.academia.edu/57658392/Optoelectronics_Research_Center?from_sitemaps=true&version=2

[38] Zimmermann, Horst. (2004). Silicon Optoelectronic Integrated Circuits. DOI: 10.1007/978-3-662-09904-9.

[39] A. Palavicini and C. Wang, "Infrared Transmission in PSi Multilayers," Optics and Photonics Journal, Vol. 3 No. 2A, 2013, pp. 20-25. DOI: 10.4236/opj.2013.32A003.

[40] Integration of periodic, sub-wavelength structures in silicon-on-insulator photonic device design. Yannick D'Mello,Orad Reshef,Santiago Bernal,Eslam El-fiky,Yun Wang,Maxime Jacques,David V. Plant. DOI: https://doi.org/10.1049/iet-opt.2019.0077

[41] The typical structural evolution of silicon anode. Lei Zhang, MohammadAl-Mamun, Liang Wang, Yuhai Dou, Longbing Qu, Shi Xue Dou, Hua KunLiu, Huijun Zhao. DOI: https://doi.org/10.1016/j.xcrp.2022.100811.

[42] Porous Silicon Gettering . I. Kuzma, Hariharsudan Sivaramakrishnan Radhakrishnan. https://www.researchgate.net/publication/278704682_Porous_Silicon_Gettering

[43] Bilyalov, Renat & Stalmans, L & Beaucarne, Guy & Loo, R. & Caymax, Matty & Poortmans, J. & Nijs, J. (2001). Porous silicon as an intermediate layer for thin-film solar cell. Solar Energy Materials and Solar Cells. 65. 477-485. DOI: 10.1016/S0927-0248(00)00130-6.

[44] Mesoporous silica nanoparticles for therapeutic/diagnostic applications. Samira Jafari, Hossein Derakhshankhah, Loghman Alaei, Ali Fattahi, Behrang Shiri Varnamkhasti, Ali Akbar Saboury. DOI: https://doi.org/10.1016/j.biopha.2018.10.167

[45] Scaffold for tissue fabrication. Peter X Ma. DOI: https://doi.org/10.1016/S1369-7021(04)00233-0

[46] SEM. Wikipedia. https://en.wikipedia.org/wiki/Scanning_electron_microscope.

[47] The effects of poly(dimethylsiloxane) surface silanization on the mesenchymal stem cell fate. Yon Jin Chuah,a Shreyas Kuddannaya,b Min Hui Adeline Lee,a Yilei Zhangb and Yuejun Kanga. DOI: 10.1039/c4bm00268g.

[48] Hydrogen Fluoride. Wikipedia. https://en.wikipedia.org/wiki/Hydrogen_fluoride

[49] Dimethylformamide. Wikipedia. https://en.wikipedia.org/wiki/Dimethylformamide

[50] Polydimethylsiloxane. Wikipedia. https://en.wikipedia.org/wiki/Polydimethylsiloxane

[51] PLGA. Wikipedia. https://en.wikipedia.org/wiki/PLGA

[52] Dichloromethane. Wikipedia. https://en.wikipedia.org/wiki/Dichloromethane

[53] Ethanol. Wikipedia. https://en.wikipedia.org/wiki/Ethanol

[54] (3-Aminopropyl)triethoxysilane. Wikipedia. https://en.wikipedia.org/wiki/(3-Aminopropyl)triethoxysilane

[55] Glutaraldehyde. Wikipedia. https://en.wikipedia.org/wiki/Glutaraldehyde

[56] Collagen. Wikipedia. https://en.wikipedia.org/wiki/Collagen

[57] Effects of SiO2 micropillar arrays on endothelial cells' morphology. Pilar Formentín, Úrsula Catalán, María Alba, Sara Fernández-Castillejo, Rosa Solà, Josep Pallarès, Lluís F. Marsal. http://dx.doi.org/10.1016/j.nbt.2016.07.002

[58] Surface Chemical Modification of Poly(dimethylsiloxane) for the Enhanced Adhesion and Proliferation of Mesenchymal Stem Cells. Shreyas Kuddannaya, Yon Jin Chuah, Min Hui Adeline Lee, Nishanth V. Menon, Yuejun Kang, and Yilei Zhang. DOI: dx.doi.org/10.1021/am402903e

[59] Bartali, Ruben & Morganti, Elisa & Lorenzelli, Leandro & Victor, Micheli & Gottardi, Gloria & Scarpa, Marina & Safeen, Mian Kashif & Pandiyan, Rajesh & Laidani, Nadhira. (2017). Oxygen plasma treatments of polydimethylsiloxane surfaces: Effect of the atomic oxygen on capillary flow in the microchannels. Micro & Nano Letters. 12. DOI: 10.1049/mnl.2017.0230.

[60] Bodin-Thomazo, Noémie & Malloggi, Florent & Guenoun, Patrick. (2017). Marker patterning: A spatially resolved method for tuning the wettability of PDMS. RSC Adv.. 7. DOI: 46514-46519. 10.1039/C7RA05654K.

[61] Redefining the importance of polylactide-co-glycolide acid (PLGA) in drug delivery. Y.R. Chavan, S.M. Tambe, D.D. Jain, S.V. Khairnar, P.D. Amin. DOI: https://doi.org/10.1016/j.pharma.2021.11.009.

[62] Agostini, Matteo & Greco, Gina & Cecchini, Marco. (2019). Polydimethylsiloxane (PDMS) irreversible bonding to untreated plastics and metals for microfluidics applications. APL Materials. 7. 081108. 10.1063/1.5070136.

[63] Lithography-based methods to manufacture biomaterials at small scales. Khanh T.M. Tran, Thanh D. Nguyen. DOI: https://doi.org/10.1016/j.jsamd.2016.12.001.

[64] Immunosensing by luminescence reduction in surface-modified microstructured SU-8. Pinkie Jacob Eravuchira, Malgorzata Baranowska, Chris Eckstein, Francesc Díaz, Eduard Llobet, Lluís F. Marsal, Josep Ferré-Borrull. DOI: http://dx.doi.org/10.1016/j.apsusc.2016.09.111

Annex

Equation 1. *PGLA + DCM mixing*

$$PGLA: DCM$$

$$1:9$$

$$DCM \rightarrow d = \left(\frac{m}{v}\right) \rightarrow d = 1.325 \rightarrow 1.325 = (m/v)$$

Since it is a 1:9 mix:

$$m = 1.325\ gr\ DCM$$

$$m = \frac{1.325\ gr\ DCM}{9} = 0.1472\ gr\ PGLA$$

Figure 43. The contact angle of native PDMS and PDMS-treated with oxygen plasma at different plasma working pressure [48].

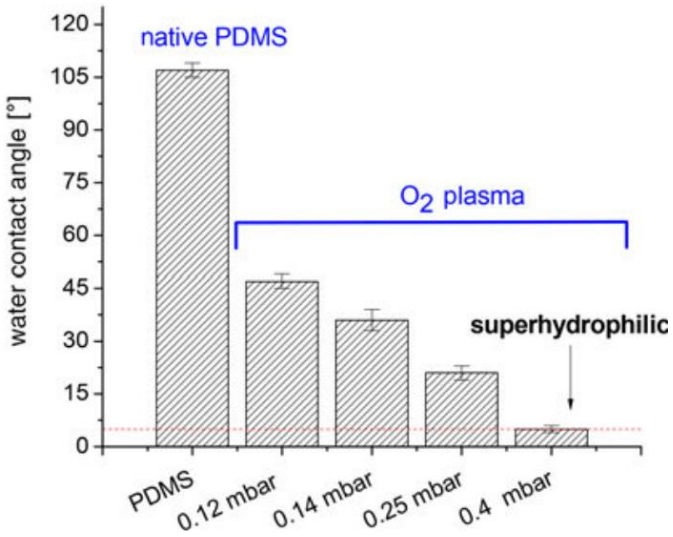

Figure 44. Evolution of the contact angle between water and PDMS as a function of the oxidation time: at the top in the areas protected by the ink, at the bottom in the unprotected areas [49].